



## An algorithm for U-Pb isotope dilution data reduction and uncertainty propagation

**N. M. McLean**

*Department of Earth, Atmospheric, and Planetary Sciences, MIT, Building 54-1126, Cambridge, Massachusetts 02139, USA (nmclean@mit.edu)*

**J. F. Bowring**

*Department of Computer Science, College of Charleston, 66 George Street, Charleston, South Carolina 29424, USA (bowringj@cofc.edu)*

**S. A. Bowring**

*Department of Earth, Atmospheric, and Planetary Sciences, MIT, Building 54-1126, Cambridge, Massachusetts 02139, USA (sbowring@mit.edu)*

[1] High-precision U-Pb geochronology by isotope dilution-thermal ionization mass spectrometry is integral to a variety of Earth science disciplines, but its ultimate resolving power is quantified by the uncertainties of calculated U-Pb dates. As analytical techniques have advanced, formerly small sources of uncertainty are increasingly important, and thus previous simplifications for data reduction and uncertainty propagation are no longer valid. Although notable previous efforts have treated propagation of correlated uncertainties for the U-Pb system, the equations, uncertainties, and correlations have been limited in number and subject to simplification during propagation through intermediary calculations. We derive and present a transparent U-Pb data reduction algorithm that transforms raw isotopic data and measured or assumed laboratory parameters into the isotopic ratios and dates geochronologists interpret without making assumptions about the relative size of sample components. To propagate uncertainties and their correlations, we describe, in detail, a linear algebraic algorithm that incorporates all input uncertainties and correlations without limiting or simplifying covariance terms to propagate them through intermediate calculations. Finally, a weighted mean algorithm is presented that utilizes matrix elements from the uncertainty propagation algorithm to propagate random and systematic uncertainties for data comparison between other U-Pb labs and other geochronometers. The linear uncertainty propagation algorithms are verified with Monte Carlo simulations of several typical analyses. We propose that our algorithms be considered by the community for implementation to improve the collaborative science envisioned by the EARTHTIME initiative.

**Components:** 18,400 words, 4 figures, 3 tables.

**Keywords:** U-Pb; geochronology; uncertainty propagation.

**Index Terms:** 1115 Geochronology: Radioisotope geochronology; 1194 Geochronology: Instruments and techniques; 1908 Informatics: Cyberinfrastructure.

**Received** 21 December 2010; **Revised** 5 April 2011; **Accepted** 5 April 2011; **Published** 24 June 2011.

McLean, N. M., J. F. Bowring, and S. A. Bowring (2011), An algorithm for U-Pb isotope dilution data reduction and uncertainty propagation, *Geochem. Geophys. Geosyst.*, 12, Q0AA18, doi:10.1029/2010GC003478.

**Theme:** EarthTime: Advances in Geochronological Technique

## 1. Introduction

[2] U-Pb geochronology by isotope dilution thermal ionization mass spectrometry (ID-TIMS) has become the gold standard for calibrating geologic time due to precisely determined uranium decay constants, high-precision measurement methods, and an internal check for open-system behavior provided by the dual decay of  $^{235}\text{U}$  and  $^{238}\text{U}$ . Precise, accurate ID-TIMS dates have been used to test and calibrate detailed tectonic models [e.g., *Schoene et al.*, 2008], determine the timing and tempo of mass extinctions and ecological recovery [*Bowring et al.*, 1998], calibrate a global geologic timescale [*Davydov et al.*, 2010], and establish a precise chronology for the early solar system [*Amelin et al.*, 2002]. These results rely on analysis and interpretation of precisely measured data, for which correct and transparent data reduction and error propagation are imperative.

[3] U-Pb ID-TIMS dates are measured by dissolving a U-bearing phase with a mixed isotopic tracer enriched in isotopes of U and Pb, then purifying the U and Pb from the resulting solution. The ratios of Pb and U in the sample to those in the tracer are measured precisely by TIMS to determine radiogenic isotope ratios of U and Pb, which are used to calculate dates. The relatively high precision of ID-TIMS dates stems from clean laboratory protocols, which minimize the magnitude and uncertainty of the laboratory blank correction, stable isotope beams with per mil level isotopic fractionation, which minimize measurement uncertainties, and well-characterized isotopic tracers, which leverage the ability of the TIMS to accurately measure isotope ratios. The accuracy of the most common geochronometer, zircon, is greatly enhanced by the chemical abrasion method, or CA-TIMS [*Mattinson*, 2005], which minimizes or eliminates any correction for loss of Pb.

[4] The last decade of developments in mass spectrometry, clean laboratory protocols, and pretreatment of zircons has increased measurement precision and decreased the magnitude of corrections for common Pb (Pbc) and open system behavior. However, the algorithms presently used for U-Pb data reduction and uncertainty propagation still maintain many simplifications and omissions better suited to past data sets. Furthermore, as random sources of uncertainty, such as ion counting statistics, have been reduced, systematic uncertainties such as calibration of the isotopic tracer have come to dominate the overall uncertainty budget.

Thus, the quality of data has outstripped the algorithms for data reduction.

[5] Several recent interlaboratory comparisons between established ID-TIMS U-Pb geochronology labs have revealed statistically significant discrepancies in measurements of the same samples. These differences likely arise from the now dominant systematic uncertainties, and represent a significant impediment to data intercomparison in collaborative science. In order to achieve the external reproducibility required by, for example timescale calibration, a common framework that transforms raw data into geological interpretation and correctly propagates systematic uncertainties is critical. The geochronology community would be well served by agreeing upon and adopting a universally accepted data reduction and uncertainty propagation algorithm for publishing and archiving data.

[6] Rather than modifying notable past data reduction and uncertainty propagation algorithms [e.g., *Ludwig*, 1980; *Roddick*, 1987; *Schmitz and Schoene*, 2007], this contribution rederives the governing equations that transform the raw data and inputs for U-Pb ID-TIMS geochronology into U-Pb and Pb-Pb dates. The equations support dating U-bearing phases with and without initial common Pb, use of several mixed U-Pb tracers, and include corrections for initial daughter isotope disequilibrium and for time-varying instrumental parameters like isotopic fractionation.

[7] A novel algorithm for propagating the input uncertainties precludes neglecting or simplifying terms in the complicated expressions for the uncertainty of U-Pb dates, thus incorporating all known sources of error. Utilizing matrices of covariance terms and partial derivatives, the uncertainty propagation algorithm also determines the statistical relationships between the U-Pb and Pb-Pb dates and is capable of breaking down the uncertainty contributions from individual sources. Contributions to the combined uncertainty from random and systematic components can then be propagated separately for each analysis, including only those systematic uncertainties necessary to compare data sets. This algorithm is extensible, so that it can accommodate future improvements in analytical methods and the uncertainty correlations arising from tracer calibrations or intercalibrated U decay constants.

[8] Data reduction and uncertainty propagation algorithms are packaged in the open-source, publicly distributed program U-Pb\_Redux, which includes a laboratory workflow manager and an interactive graphical user interface that performs

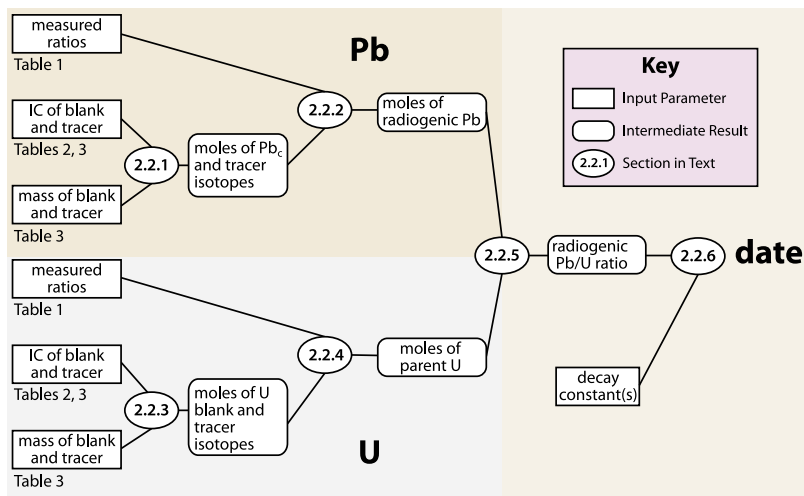


**Figure 1.** Diagrammatic representation of the data reduction algorithm. Data reduction begins with the input parameters in the boxes at left. Sections 2.2.1 and 2.2.3 describe how the blank and tracer parameters are combined to calculate their molar abundances. These are then used to correct the measured ratios in sections 2.2.2 and 2.2.4 in order to determine the moles of parent Pb and radiogenic U, respectively. Finally, sections 2.2.5 and 2.2.6 calculate radiogenic U/Pb ratios and, using the isotopic decay constants, isotopic dates.

statistical calculations and plotting [Bowring *et al.*, 2011]. U-Pb\_Redux is also capable of exporting all of the calculated dates, interpretations, and supporting data to an online database, then downloading data sets for further interpretation and compilation with new data from multiple users. Community adoption of a common, transparent algorithm like the one in U-Pb\_Redux would ensure that data from different users in different labs can be compared and combined.

## 2. U-Pb Data Reduction

[9] A number of corrections and calculations are required to transform measured isotopic ratios and lab parameters into meaningful isotopic dates, as illustrated in Figure 1. If isobaric interferences are present, they must be measured and subtracted before each isotope ratio is corrected for instrumental mass fractionation, or mass bias, caused by lighter isotopes evaporating and ionizing more easily than heavier isotopes. The numerator and denominator of a measured, corrected isotope ratio then represent mixtures of multiple components: the parent or radiogenic daughter isotope; the isotopic tracer used; common Pb and U added during laboratory procedures, known as laboratory blank; and if present, initial common Pb incorporated during crystallization of the phase (Figure 2).

[10] There are three ways to calculate isotopic dates from fractionation- and interference-corrected ratios.

If the isotopic composition (IC) of the common Pb components are known, they may be subtracted along with the tracer contribution to directly determine radiogenic isotope ratios; along with appropriate decay constants, these determine the isotopic date. Alternatively, after subtracting the estimated laboratory blank and isotopic tracer contributions, the resulting isotope ratios may represent variable mixtures of a single initial common Pb isotopic composition and an amount of radiogenic Pb proportional to the amount of parent isotope present. Assuming a closed system, both the sample date and the isotopic composition of the initial common Pb can be calculated using an isochron technique. Finally, a linear regression through discordant U-Pb analyses can be extrapolated to concordia intercepts that may be interpreted in terms of a single episode of open system behavior.

[11] This section explores the inputs required and the mechanism used for accurate U-Pb data reduction. Text accompanying each equation in the data reduction algorithm explains its applicability and purpose.

### 2.1. Inputs

[12] A weighted mean, isochron, or concordia intercept date is calculated from a number of paired U and Pb analyses, here termed ‘fractions’ [Bowring *et al.*, 2011]. Examples include single mineral grains or grain fragments, as well as a bulk leach or a whole

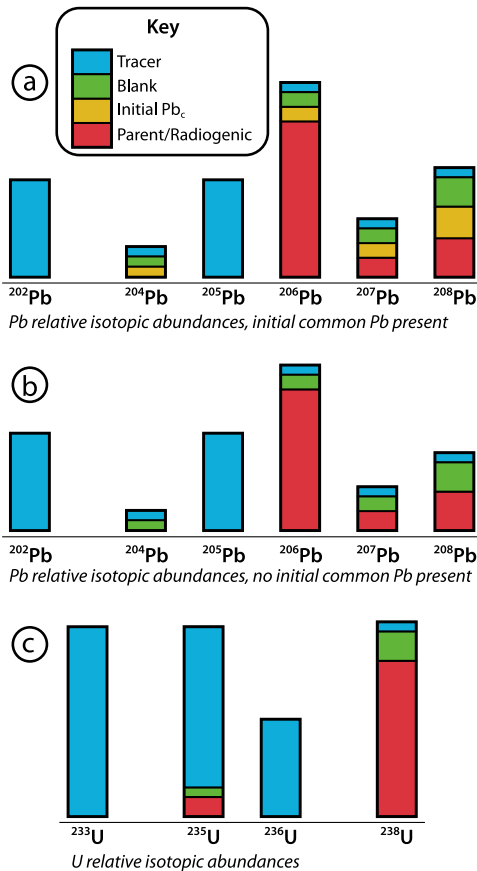


**Figure 2.** Cartoon illustrating the relative contributions of Pb and U sample components for typical U-Pb ID-TIMS analyses, broken down by isotope. Column heights are not shown to scale. (a) Relative abundance of Pb isotopes in a phase that incorporates initial common Pb (Pbc). Determination of the radiogenic  $^{206}\text{Pb}$ ,  $^{207}\text{Pb}$ , and  $^{208}\text{Pb}$  shown in red requires subtracting the tracer, blank, and initial Pbc contributions from the top of each column. The tracer contribution is estimated from the  $^{205}\text{Pb}$  abundance and the tracer isotopic composition (IC), and the Pb blank contribution is estimated laboratory measurements. The remaining  $^{204}\text{Pb}$  is assumed to be initial Pbc; its contributions to the radiogenic isotopes are subtracted using the initial Pbc IC, leaving only the radiogenic component. (b) For a phase with no initial Pbc, only tracer and blank contributions need to be subtracted to determine the radiogenic component. The  $^{204}\text{Pb}$  contribution from the tracer is subtracted first using the  $^{205}\text{Pb}$  abundance of the tracer, and the remaining  $^{204}\text{Pb}$  is assumed to be laboratory Pb blank. Subtracting the blank contributions to  $^{206}\text{Pb}$ ,  $^{207}\text{Pb}$ , and  $^{208}\text{Pb}$  using the blank IC yields their radiogenic components. (c) Relative abundance of U isotopes. The isotopic tracer may contain any combination of  $^{233}\text{U}$ ,  $^{235}\text{U}$ , and/or  $^{236}\text{U}$ . The tracer, blank, and sample U contributions to each isotope are deconvolved by solving a system of equations that incorporates the IC of each.

**Table 1.** Measured Isotope Ratios

Pb	U or Uoxide
$\left(\frac{^{204}\text{Pb}}{^{205}\text{Pb}}\right)_{meas}$	$\left(\frac{^{233}\text{U}}{^{235}\text{U}}\right)_{meas}$ OR $\left(\frac{^{265}\text{UO}_2}{^{267}\text{UO}_2}\right)_{meas}$
$\left(\frac{^{206}\text{Pb}}{^{205}\text{Pb}}\right)_{meas}$	$\left(\frac{^{238}\text{U}}{^{235}\text{U}}\right)_{meas}$ OR $\left(\frac{^{270}\text{UO}_2}{^{267}\text{UO}_2}\right)_{meas}$
$\left(\frac{^{207}\text{Pb}}{^{205}\text{Pb}}\right)_{meas}$	$\left(\frac{^{233}\text{U}}{^{236}\text{U}}\right)_{meas}$ OR $\left(\frac{^{265}\text{UO}_2}{^{268}\text{UO}_2}\right)_{meas}$
$\left(\frac{^{208}\text{Pb}}{^{205}\text{Pb}}\right)_{meas}$	$\left(\frac{^{238}\text{U}}{^{236}\text{U}}\right)_{meas}$ OR $\left(\frac{^{270}\text{UO}_2}{^{268}\text{UO}_2}\right)_{meas}$
$\left(\frac{^{202}\text{Pb}}{^{205}\text{Pb}}\right)_{meas}$	

rock analysis. Between twenty and forty separate input variables are required to calculate an isotopic date for each fraction, and each is described below. These inputs, as well as the symbols used to represent them in the following data reduction algorithm, are listed in Tables 1–3.

[13] All data must be reduced with a self-consistent set of physical constants, such as decay constants and atomic masses. Decay constants used for isotopic date calculation and disequilibrium correction include those for  $^{231}\text{Pa}$ ,  $^{230}\text{Th}$ ,  $^{232}\text{Th}$ ,  $^{235}\text{U}$ , and  $^{238}\text{U}$ . The atomic masses of the isotopes, which are the only inputs not assigned an uncertainty, are used to convert between masses and moles of elements or isotopes.

[14] An isotopic tracer is a mixture of well-determined quantities of enriched isotopes. The equations presented here apply to the most commonly used isotopic tracers for U-Pb ID-TIMS geochronology, which are enriched in either  $^{205}\text{Pb}$  or both  $^{202}\text{Pb}$  and  $^{205}\text{Pb}$ , as well as either  $^{235}\text{U}$ , both  $^{233}\text{U}$  and  $^{235}\text{U}$ , or both  $^{233}\text{U}$  and  $^{236}\text{U}$ . In addition to the enriched isotopes, tracer solutions inevitably contain minor amounts of other naturally occurring isotopes, whose proportions must be known for full characterization of the U and Pb IC of the tracer. Finally, isotope dilution calculations utilize the concentrations of the artificial Pb and U isotopes (Table 2).

[15] Fractions analyzed on the same mass spectrometer with the same laboratory procedures will have additional parameters in common. For elements with at least two enriched isotopes present in

**Table 2.** Isotopic Tracer Parameters

Pb IC	U IC	Tracer Calibration
$\left(\frac{^{204}\text{Pb}}{^{205}\text{Pb}}\right)_{tr}$	$\left(\frac{^{233}\text{U}}{^{235}\text{U}}\right)_{tr}$	$\left(\frac{^{205}\text{Pb}}{^{235}\text{U}}\right)_{tr}$
$\left(\frac{^{206}\text{Pb}}{^{205}\text{Pb}}\right)_{tr}$	$\left(\frac{^{238}\text{U}}{^{235}\text{U}}\right)_{tr}$	$conc(^{205}\text{Pb})_{tr}$
$\left(\frac{^{207}\text{Pb}}{^{205}\text{Pb}}\right)_{tr}$	$\left(\frac{^{233}\text{U}}{^{236}\text{U}}\right)_{tr}$	$conc(^{235}\text{U})_{tr}$
$\left(\frac{^{208}\text{Pb}}{^{205}\text{Pb}}\right)_{tr}$		$mass_{tr}$
$\left(\frac{^{202}\text{Pb}}{^{205}\text{Pb}}\right)_{tr}$		

**Table 3.** Laboratory and Sample Parameters

Pb Blank	Initial Pb <sub>c</sub>	Uranium
$\left(\frac{^{206}\text{Pb}}{^{204}\text{Pb}}\right)_{bl}$	$\left(\frac{^{206}\text{Pb}}{^{204}\text{Pb}}\right)_{com}$	$\left(\frac{^{238}\text{U}}{^{235}\text{U}}\right)_{spl}$
$\left(\frac{^{207}\text{Pb}}{^{204}\text{Pb}}\right)_{bl}$	$\left(\frac{^{207}\text{Pb}}{^{204}\text{Pb}}\right)_{com}$	$\left(\frac{^{238}\text{U}}{^{235}\text{U}}\right)_{bl}$
$\left(\frac{^{208}\text{Pb}}{^{204}\text{Pb}}\right)_{bl}$	$\left(\frac{^{208}\text{Pb}}{^{204}\text{Pb}}\right)_{com}$	$\left(\frac{^{18}\text{O}}{^{16}\text{O}}\right)_{Uox}$
$mass(\text{Pb})_{bl}$	$t_{Pbc}$	$mass(\text{U})_{bl}$
Fractionation Correction	Disequilibrium Correction	Physical Constants
$\alpha_{\text{Pb}}$	$\left(\frac{\text{Th}}{\text{U}}\right)_{magma}$	$\lambda_{238}, \lambda_{235}, \lambda_{232}, \lambda_{231}, \lambda_{230}$
$\alpha_{\text{U}}$	$\left[\frac{^{231}\text{Pa}}{^{233}\text{U}}\right]_{spl}$	$\left[\frac{\text{grams}(^{204}\text{Pb})}{\text{mole}(^{204}\text{Pb})}\right]$

the tracer, isotopic fractionation during each run can be calculated either on average or point-by-point by comparing the known ratio to the measured ratio (see sections 2.2.1.1, 2.2.4.1, and 2.2.4.3). However, if only one enriched isotope is present (e.g., a single  $^{205}\text{Pb}$  or  $^{235}\text{U}$  tracer), the magnitude and variability of mass-dependent fractionation must be assessed by repeated analyses of a standard for input to data reduction. A linear fractionation law is used here for ID-TIMS analyses, which is virtually indistinguishable from an exponential or power law correction at low (ca. 0.1% per u) magnitudes of isotopic fractionation.

[16] Two methods to allocate common Pb are implemented in U-Pb\_Redux. The first assumes that all common Pb (Pbc) in the analysis is laboratory blank. This assumption is justified when total procedural blank measurements are the same magnitude as the total common Pb measurements of analyses, as demonstrated for chemically abraded zircon [e.g., *Davydov et al.*, 2010]. The laboratory blank isotopic composition should be measured for each sample preparation procedure (e.g., HCl- vs. HBr-based anion exchange chemistry), then subtracted from each analysis, as described in sections 2.2.1.3 and 2.2.1.2.

[17] When the dated phase contains initial common Pb, its IC can be determined in one of three ways. With no a priori knowledge, a terrestrial Pb ore model like that of *Stacey and Kramers* [1975] or *Cumming and Richards* [1975] can be used to estimate its IC, using the approximate age of the sample. Leaching experiments on comagmatic low-U phases such as alkali feldspar, if present, can precisely determine the initial common Pb IC [*Housh and Bowring*, 1991]. Finally, if several fractions formed closed systems at the same time, share the same initial Pb isotopic composition, and remained closed systems until analysis, then an isochron approach

may be used to solve for both their initial common Pb IC and date simultaneously.

[18] Several additional parameters are needed to reduce U data (Table 3). Unless it has been determined independently, the user must specify the  $^{238}\text{U}/^{235}\text{U}$  ratio of the sample. Canonically, this value has been accepted as 137.88 [*Steiger and Jager*, 1977], but recent studies have shown that it may vary significantly in nature [*Stirling et al.*, 2007; *Weyer et al.*, 2008; *Brennecke et al.*, 2010]. The mass and the  $^{238}\text{U}/^{235}\text{U}$  ratio of the U blank are also necessary. Finally, if the U is measured as a  $\text{UO}_2^+$  species with a mixed  $^{233}\text{U}$ - $^{235}\text{U}$  tracer, the  $^{18}\text{O}/^{16}\text{O}$  ratio of the uranium oxide is used to correct for the isobaric interferences of  $^{233}\text{U}^{16}\text{O}^{18}\text{O}$  or  $^{233}\text{U}^{16}\text{O}^{18}\text{O}$  on  $^{235}\text{U}^{16}\text{O}^{16}\text{O}$ .

[19] Initial isotopic disequilibrium in either the  $^{238}\text{U}$  or  $^{235}\text{U}$  decay chains can result in systematic errors due to excess or deficit radiogenic daughter. In U-Pb geochronology, it is often assumed that the magma from which the dated phase crystallized was close to secular equilibrium. As the phase crystallizes, it may preferentially incorporate or exclude an intermediate daughter element from the  $^{238}\text{U}$  or  $^{235}\text{U}$  decay chain. For instance, monazite preferentially incorporates  $^{230}\text{Th}$  in the  $^{238}\text{U}$  decay chain [*Schärer*, 1984], while zircon excludes it [*Mattinson*, 1973], resulting in enrichment or depletion in  $^{206}\text{Pb}$ , respectively. The magnitude of the disequilibrium correction is modeled using the  $^{208}\text{Pb}$  content of a mineral to determine its Th/U ratio, then comparing to a user input Th/U ratio of the magma. Another long-lived intermediate daughter isotope is  $^{231}\text{Pa}$ , in the  $^{235}\text{U}$  decay chain. Because there is no abundant long-lived Pa isotope, the initial  $^{231}\text{Pa}/^{235}\text{U}$  activity ratio or the ratio of Pa and U distribution coefficients must be input by the user to make this correction, described in Appendix A.

[20] Although multiple analyses may share many of the above parameters, each will have a unique set of measured Pb and U ratios. The measured ratios are the same as those needed for tracer characterization: the ratio of each naturally occurring isotope to a tracer isotope, and if multiple enriched isotopes are present, their ratio to one another (Table 1). The mass of tracer solution added to the analysis before measurement is also required to calculate the molar quantities of the sample and tracer isotopes.

## 2.2. Data Reduction

[21] The algorithm that transforms the input parameters into isotopic dates can be broken down into

three stages: Pb calculations, U calculations, and isotopic date determination. Each category entails calculation of multiple intermediate parameters, and the algorithm depends upon the tracer used and whether or not initial common Pb is present. Figure 1 illustrates the data reduction algorithm as a flow chart, with numbered ovals corresponding to the text section where each calculation appears.

### 2.2.1. Pb Calculations

[22] The Pb calculations are detailed in the top left panel of Figure 1 and the ovals contain section references to the text that follows.

#### 2.2.1.1. Tracer

[23] Isotope dilution uses a known quantity of a synthetic tracer isotope to determine the unknown amount of sample present.  $^{205}\text{Pb}$  is ubiquitously used as the artificially enriched Pb isotope, and its abundance can be calculated from the measured mass of the tracer and its known concentration of  $^{205}\text{Pb}$ .

$$\text{moles}(^{205}\text{Pb})_{tr} = \text{conc}(^{205}\text{Pb})_{tr} \cdot \text{mass}_{tr} \quad (1)$$

[24] If a  $^{202}\text{Pb}$ - $^{205}\text{Pb}$  tracer is used, the linear isotopic fractionation factor  $\alpha_{Pb}$  is proportional to the difference between the measured and true  $^{202}\text{Pb}/^{205}\text{Pb}$  ratios.

$$\alpha_{Pb} = \frac{1}{3} \left[ 1 - \left( \frac{^{202}\text{Pb}}{^{205}\text{Pb}} \right)_{tr} / \left( \frac{^{202}\text{Pb}}{^{205}\text{Pb}} \right)_{meas} \right] \quad (2)$$

If a tracer containing only  $^{205}\text{Pb}$  is used, then  $\alpha_{Pb}$  must be determined from repeated measurements of an isotopic standard, such as NBS981 or NBS982, or from other analyses with the  $^{202}\text{Pb}$ - $^{205}\text{Pb}$  tracer.

[25] Because  $^{204}\text{Pb}$  has no radiogenic component, the fractionation-corrected  $^{204}\text{Pb}/^{205}\text{Pb}$  ratio can be used to determine the mass of common Pb (Pbc). Figure 2 illustrates the relationship between sample Pb components.

$$\left( \frac{^{204}\text{Pb}}{^{205}\text{Pb}} \right)_{fc} = \left( \frac{^{204}\text{Pb}}{^{205}\text{Pb}} \right)_{meas} \cdot (1 - \alpha_{Pb}) \quad (3)$$

#### 2.2.1.2. Laboratory Blank and Initial Common Pb

[26] If initial common Pb is present, then the  $^{204}\text{Pb}$  in the analysis must be apportioned between tracer, laboratory blank, and initial common Pb contributions. These relative contributions are illustrated in Figure 2a. When the isotopic composition of the initial common Pb has not been or cannot be mea-

sured directly, a popular alternative, albeit imperfect, is to use a Pb ore evolution model such as that of *Stacey and Kramers* [1975], which is reproduced in Appendix A.

[27] When initial common Pb is present, the total common Pb is apportioned by assuming the mass of the laboratory Pb blank, usually an average of several contemporaneous total procedural blank measurements. To calculate the moles of each isotope present from its mass and isotopic composition, it is helpful to first calculate the grams of laboratory Pb blank per mole of  $^{204}\text{Pb}$  in the blank:

$$\left[ \frac{\text{grams}(\text{Pb})}{\text{mole}(^{204}\text{Pb})} \right]_{bl} = \frac{\text{grams}(^{204}\text{Pb})}{\text{mole}(^{204}\text{Pb})} + \left( \frac{^{206}\text{Pb}}{^{204}\text{Pb}} \right)_{bl} \cdot \frac{\text{grams}(^{206}\text{Pb})}{\text{mole}(^{206}\text{Pb})} + \left( \frac{^{207}\text{Pb}}{^{204}\text{Pb}} \right)_{bl} \cdot \frac{\text{grams}(^{207}\text{Pb})}{\text{mole}(^{207}\text{Pb})} + \left( \frac{^{208}\text{Pb}}{^{204}\text{Pb}} \right)_{bl} \cdot \frac{\text{grams}(^{208}\text{Pb})}{\text{mole}(^{208}\text{Pb})} \quad (4)$$

[28] The moles of  $^{204}\text{Pb}$  in the laboratory blank can now be determined from the blank mass input by the user,

$$\text{moles}(^{204}\text{Pb})_{bl} = \text{mass}(\text{Pb})_{bl} / \left[ \frac{\text{grams}(\text{Pb})}{\text{mole}(^{204}\text{Pb})} \right]_{bl} \quad (5)$$

and the moles  $^{206}\text{Pb}$ ,  $^{207}\text{Pb}$ , and  $^{208}\text{Pb}$  in the laboratory blank are computed using (5) and the Pb blank IC.

$$\text{moles}(^{206}\text{Pb})_{bl} = \frac{\left( \frac{^{206}\text{Pb}}{^{204}\text{Pb}} \right)_{bl} \cdot \text{mass}(\text{Pb})_{bl}}{\left[ \frac{\text{grams}(\text{Pb})}{\text{mole}(^{204}\text{Pb})} \right]_{bl}} \quad (6)$$

$$\text{moles}(^{207}\text{Pb})_{bl} = \frac{\left( \frac{^{207}\text{Pb}}{^{204}\text{Pb}} \right)_{bl} \cdot \text{mass}(\text{Pb})_{bl}}{\left[ \frac{\text{grams}(\text{Pb})}{\text{mole}(^{204}\text{Pb})} \right]_{bl}} \quad (7)$$

$$\text{moles}(^{208}\text{Pb})_{bl} = \frac{\left( \frac{^{208}\text{Pb}}{^{204}\text{Pb}} \right)_{bl} \cdot \text{mass}(\text{Pb})_{bl}}{\left[ \frac{\text{grams}(\text{Pb})}{\text{mole}(^{204}\text{Pb})} \right]_{bl}} \quad (8)$$

[29] The total molar quantity of  $^{204}\text{Pb}$  from common Pb, composed of both initial common Pb and laboratory blank, is the total moles of  $^{204}\text{Pb}$  analyzed minus the contribution from the tracer.

$$\text{moles}(^{204}\text{Pb})_{ic} = \text{moles}(^{205}\text{Pb})_{tr} \cdot \left[ \left( \frac{^{204}\text{Pb}}{^{205}\text{Pb}} \right)_{fc} - \left( \frac{^{204}\text{Pb}}{^{205}\text{Pb}} \right)_{tr} \right] \quad (9)$$

[30] Because the total common Pb is composed of laboratory blank Pb and initial Pbc, the additional  $^{204}\text{Pb}$  in excess of the laboratory blank is assumed to be initial Pbc.

$$\text{moles}^{(204}\text{Pb})_{\text{com}} = \text{moles}^{(204}\text{Pb})_{\text{ic}} - \text{moles}^{(204}\text{Pb})_{\text{bl}} \quad (10)$$

[31] The initial Pbc contributions to other Pb isotopes can be calculated from the initial  $^{204}\text{Pb}$  using the initial common Pb IC determined by the user or from a model, such as equations (A25) to (A30).

$$\text{moles}^{(206}\text{Pb})_{\text{com}} = \left(\frac{^{206}\text{Pb}}{^{204}\text{Pb}}\right)_{\text{com}} \cdot \text{moles}^{(204}\text{Pb})_{\text{com}} \quad (11)$$

$$\text{moles}^{(207}\text{Pb})_{\text{com}} = \left(\frac{^{207}\text{Pb}}{^{204}\text{Pb}}\right)_{\text{com}} \cdot \text{moles}^{(204}\text{Pb})_{\text{com}} \quad (12)$$

$$\text{moles}^{(208}\text{Pb})_{\text{com}} = \left(\frac{^{208}\text{Pb}}{^{204}\text{Pb}}\right)_{\text{com}} \cdot \text{moles}^{(204}\text{Pb})_{\text{com}} \quad (13)$$

### 2.2.1.3. Laboratory Blank, No Initial Common Pb

[32] When the dated phase incorporates no initial common Pb, the moles of  $^{204}\text{Pb}$  in the laboratory blank can be expressed as the total moles of  $^{204}\text{Pb}$  in the analysis minus any contribution from the tracer (Figure 2b). The moles of  $^{204}\text{Pb}$  in the laboratory blank, along with its average isotopic composition, are then used to calculate the moles of  $^{206}\text{Pb}$ ,  $^{207}\text{Pb}$ , and  $^{208}\text{Pb}$  in the laboratory blank.

$$\text{moles}^{(204}\text{Pb})_{\text{bl}} = \text{moles}^{(205}\text{Pb})_{\text{tr}} \cdot \left[ \left(\frac{^{204}\text{Pb}}{^{205}\text{Pb}}\right)_{\text{fc}} - \left(\frac{^{204}\text{Pb}}{^{205}\text{Pb}}\right)_{\text{tr}} \right] \quad (14)$$

$$\begin{aligned} \text{moles}^{(206}\text{Pb})_{\text{bl}} &= \text{moles}^{(205}\text{Pb})_{\text{tr}} \cdot \left(\frac{^{206}\text{Pb}}{^{204}\text{Pb}}\right)_{\text{bl}} \\ &\cdot \left[ \left(\frac{^{204}\text{Pb}}{^{205}\text{Pb}}\right)_{\text{fc}} - \left(\frac{^{204}\text{Pb}}{^{205}\text{Pb}}\right)_{\text{tr}} \right] \end{aligned} \quad (15)$$

$$\begin{aligned} \text{moles}^{(207}\text{Pb})_{\text{bl}} &= \text{moles}^{(205}\text{Pb})_{\text{tr}} \cdot \left(\frac{^{207}\text{Pb}}{^{204}\text{Pb}}\right)_{\text{bl}} \\ &\cdot \left[ \left(\frac{^{204}\text{Pb}}{^{205}\text{Pb}}\right)_{\text{fc}} - \left(\frac{^{204}\text{Pb}}{^{205}\text{Pb}}\right)_{\text{tr}} \right] \end{aligned} \quad (16)$$

$$\begin{aligned} \text{moles}^{(208}\text{Pb})_{\text{bl}} &= \text{moles}^{(205}\text{Pb})_{\text{tr}} \cdot \left(\frac{^{208}\text{Pb}}{^{204}\text{Pb}}\right)_{\text{bl}} \\ &\cdot \left[ \left(\frac{^{204}\text{Pb}}{^{205}\text{Pb}}\right)_{\text{fc}} - \left(\frac{^{204}\text{Pb}}{^{205}\text{Pb}}\right)_{\text{tr}} \right] \end{aligned} \quad (17)$$

The total mass of laboratory blank Pb, frequently reported in data tables, should be calculated from the

moles of Pb isotopes in the blank and their gram atomic masses.

### 2.2.2. Radiogenic and Sample Pb

[33] The tracer IC, along with the moles of laboratory blank and initial Pbc, provide enough information to determine the radiogenic components of  $^{206}\text{Pb}$ ,  $^{207}\text{Pb}$ , and  $^{208}\text{Pb}$  in the analysis. First, the measured ratios of Pb isotopes relative to  $^{205}\text{Pb}$  in the tracer are fractionation corrected, and the tracer contribution is subtracted. Multiplying this by the moles of  $^{205}\text{Pb}$  in the tracer gives the molar quantity of each Pb isotope in the sample, from which the Pb blank and initial Pbc components are subtracted.

$$\begin{aligned} \text{moles}^{(206}\text{Pb})_{\text{rad}} &= \text{moles}^{(205}\text{Pb})_{\text{tr}} \\ &\cdot \left[ \left(\frac{^{206}\text{Pb}}{^{205}\text{Pb}}\right)_{\text{meas}} \cdot (1 + \alpha_{\text{Pb}}) - \left(\frac{^{206}\text{Pb}}{^{205}\text{Pb}}\right)_{\text{tr}} \right] \\ &- \text{moles}^{(206}\text{Pb})_{\text{bl}} - \text{moles}^{(206}\text{Pb})_{\text{com}} \end{aligned} \quad (18)$$

$$\begin{aligned} \text{moles}^{(207}\text{Pb})_{\text{rad}} &= \text{moles}^{(205}\text{Pb})_{\text{tr}} \\ &\cdot \left[ \left(\frac{^{207}\text{Pb}}{^{205}\text{Pb}}\right)_{\text{meas}} \cdot (1 + 2\alpha_{\text{Pb}}) - \left(\frac{^{207}\text{Pb}}{^{205}\text{Pb}}\right)_{\text{tr}} \right] \\ &- \text{moles}^{(207}\text{Pb})_{\text{bl}} - \text{moles}^{(207}\text{Pb})_{\text{com}} \end{aligned} \quad (19)$$

$$\begin{aligned} \text{moles}^{(208}\text{Pb})_{\text{rad}} &= \text{moles}^{(205}\text{Pb})_{\text{tr}} \\ &\cdot \left[ \left(\frac{^{208}\text{Pb}}{^{205}\text{Pb}}\right)_{\text{meas}} \cdot (1 + 3\alpha_{\text{Pb}}) - \left(\frac{^{208}\text{Pb}}{^{205}\text{Pb}}\right)_{\text{tr}} \right] \\ &- \text{moles}^{(208}\text{Pb})_{\text{bl}} - \text{moles}^{(208}\text{Pb})_{\text{com}} \end{aligned} \quad (20)$$

[34] If an isochron technique is employed, the initial Pbc isotopic composition for a group of fractions is calculated or constrained at the same time as their date. Only the common Pb from the laboratory blank and tracer should be subtracted in this case, leaving the mass of each isotope of Pb from the sample.

$$\begin{aligned} \text{moles}^{(206}\text{Pb})_{\text{spl}} &= \text{moles}^{(205}\text{Pb})_{\text{tr}} \\ &\cdot \left[ \left(\frac{^{206}\text{Pb}}{^{205}\text{Pb}}\right)_{\text{meas}} \cdot (1 + \alpha_{\text{Pb}}) - \left(\frac{^{206}\text{Pb}}{^{205}\text{Pb}}\right)_{\text{tr}} \right] - \text{moles}^{(206}\text{Pb})_{\text{bl}} \end{aligned} \quad (21)$$

$$\begin{aligned} \text{moles}^{(207}\text{Pb})_{\text{spl}} &= \text{moles}^{(205}\text{Pb})_{\text{tr}} \\ &\cdot \left[ \left(\frac{^{207}\text{Pb}}{^{205}\text{Pb}}\right)_{\text{meas}} \cdot (1 + 2\alpha_{\text{Pb}}) - \left(\frac{^{207}\text{Pb}}{^{205}\text{Pb}}\right)_{\text{tr}} \right] - \text{moles}^{(207}\text{Pb})_{\text{bl}} \end{aligned} \quad (22)$$

$$\begin{aligned} \text{moles}^{(208}\text{Pb})_{\text{spl}} &= \text{moles}^{(205}\text{Pb})_{\text{tr}} \\ &\cdot \left[ \left(\frac{^{208}\text{Pb}}{^{205}\text{Pb}}\right)_{\text{meas}} \cdot (1 + 3\alpha_{\text{Pb}}) - \left(\frac{^{208}\text{Pb}}{^{205}\text{Pb}}\right)_{\text{tr}} \right] - \text{moles}^{(208}\text{Pb})_{\text{bl}} \end{aligned} \quad (23)$$

### 2.2.3. U Calculations

[35] The U calculations are detailed in the bottom left panel of Figure 1 and the ovals contain section references to the text that follows.

#### 2.2.3.1. Oxide Correction

[36] Uranium is commonly measured by TIMS in two forms, as a metal ( $U^+$ ) species, or as an oxide ( $UO_2^+$ ). Although the oxide species ionizes more efficiently, it introduces possible isobaric interferences. About 99.8% of oxygen is  $^{16}O$  and 0.2% is  $^{18}O$ . Using a mixed  $^{233}U$ - $^{235}U$  tracer, the  $^{18}O$  creates a significant isobaric interference:  $^{233}U^{18}O^{16}O$  (mass = 267) on  $^{235}U^{16}O^{16}O$  (mass = 267). Because both  $U^{18}O^{16}O$  and  $U^{16}O^{18}O$  permutations are possible, the  $^{233}UO_2$  with one  $^{18}O$  will be approximately  $(0.2\% \text{ } ^{18}O \text{ abundance}) \times (2 \text{ } UO_2 \text{ permutations}) = 0.4\%$  as abundant as  $^{233}U^{16}O^{16}O$ . The precise correction depends on the  $^{18}O/^{16}O$  in the  $UO_2^+$  species, which can be measured during the analysis on high-intensity ion beams, or inferred for smaller samples from the mean value of the larger runs.

[37] Because the isobaric interference is underneath the  $^{235}U$  peak, both the measured  $^{238}U/^{235}U$  oxide (mass 270/267) and  $^{233}U/^{235}U$  oxide (mass 265/267) ratios must be corrected.

$$\left(\frac{^{233}U}{^{235}U}\right)_{oc} = \frac{\left(\frac{^{265}UO_2}{^{267}UO_2}\right)_{meas}}{1 - 2\left(\frac{^{18}O}{^{16}O}\right)_{Uox} \cdot \left(\frac{^{265}UO_2}{^{267}UO_2}\right)_{meas}} \quad (24)$$

$$\left(\frac{^{238}U}{^{235}U}\right)_{oc} = \frac{\left(\frac{^{270}UO_2}{^{267}UO_2}\right)_{meas}}{1 - 2\left(\frac{^{18}O}{^{16}O}\right)_{Uox} \cdot \left(\frac{^{265}UO_2}{^{267}UO_2}\right)_{meas}} \quad (25)$$

#### 2.2.3.2. U Blank and Tracer Masses

[38] Regardless of the tracer used, the mass of both the U blank and tracer contributions are calculated from their input masses and isotopic compositions.

$$moles(^{235}U)_{bl} = \frac{mass(U)_{bl}}{\frac{grams(^{235}U)}{mole(^{235}U)} + \left(\frac{^{238}U}{^{235}U}\right)_{bl} \cdot \frac{grams(^{238}U)}{mole(^{238}U)}} \quad (26)$$

$$moles(^{238}U)_{bl} = \left(\frac{^{238}U}{^{235}U}\right)_{bl} \cdot moles(^{235}U)_{bl} \quad (27)$$

$$moles(^{235}U)_{tr} = conc(^{235}U)_{tr} \cdot mass_{tr} \quad (28)$$

$$moles(^{238}U)_{tr} = \left(\frac{^{238}U}{^{235}U}\right)_{tr} \cdot moles(^{235}U)_{tr} \quad (29)$$

[39] If the tracer contains the synthetic isotope  $^{233}U$ , then its molar quantity must also be calculated before determining the radiogenic components of the sample.

$$moles(^{233}U)_{tr} = \left(\frac{^{233}U}{^{235}U}\right)_{tr} \cdot moles(^{235}U)_{tr} \quad (30)$$

### 2.2.4. Simultaneous Fractionation Correction and Isotope Dilution

#### 2.2.4.1. Fractionation Correction and Isotope Dilution for a Mixed $^{233}U$ - $^{235}U$ Tracer

[40] Using a mixed  $^{233}U$ - $^{235}U$  tracer, such as the EARTHTIME-distributed 'ET535 tracer', requires simultaneous fractionation correction and isotope dilution, and blank and tracer subtraction calculations. This yields an expression for both the amount of parent U present and the linear fractionation factor  $\alpha_U$ .

[41] To begin, the contributions to the three measured U isotopes are (Figure 2)

$$moles(^{233}U)_{tot} = moles(^{233}U)_{tr} \quad (31)$$

$$moles(^{235}U)_{tot} = moles(^{235}U)_{tr} + moles(^{235}U)_{bl} + moles(^{235}U)_{spl} \quad (32)$$

$$moles(^{238}U)_{tot} = moles(^{238}U)_{tr} + moles(^{238}U)_{bl} + moles(^{238}U)_{spl} \quad (33)$$

[42] After fractionation correction, the oxide-corrected ratios in (24) and (25) or the  $^{233}U/^{235}U$  and  $^{238}U/^{235}U$  ratios measured as a metal represent the molar ratios of the quantities in equations (31) and (33) to those in (32).

$$\left(\frac{^{233}U}{^{235}U}\right)_{oc} \cdot (1 - 2\alpha_U) = \frac{moles(^{233}U)_{tr}}{\left[moles(^{235}U)_{tr} + moles(^{235}U)_{bl} + moles(^{235}U)_{spl}\right]} \quad (34)$$

$$\left(\frac{^{238}U}{^{235}U}\right)_{oc} \cdot (1 + 3\alpha_U) = \frac{\left[moles(^{238}U)_{tr} + moles(^{238}U)_{bl} + moles(^{238}U)_{spl}\right]}{\left[moles(^{235}U)_{tr} + moles(^{235}U)_{bl} + moles(^{235}U)_{spl}\right]} \quad (35)$$

[43] The two equations (34) and (35) have three unknowns,  $\alpha_U$  and the moles of  $^{235}U$  and  $^{238}U$ . The rest of the terms are defined in equations (26) to (30).



To eliminate a variable, the moles of  $^{238}\text{U}$  can be expressed as the moles of  $^{235}\text{U}$  multiplied by the  $^{238}\text{U}/^{235}\text{U}$  of the sample. Making this substitution and solving the system of equations for the moles of  $^{235}\text{U}$  in the sample and  $\alpha_{\text{U}}$  yields

$$\begin{aligned} \text{moles}(^{235}\text{U})_{\text{spl}} = & \left[ 3 \left( \frac{^{238}\text{U}}{^{235}\text{U}} \right)_{\text{oc}} / \left( \frac{^{233}\text{U}}{^{235}\text{U}} \right)_{\text{oc}} \cdot \text{moles}(^{233}\text{U})_{\text{tr}} \right. \\ & - 5 \left( \frac{^{238}\text{U}}{^{235}\text{U}} \right)_{\text{oc}} \cdot \left( \text{moles}(^{235}\text{U})_{\text{bl}} + \text{moles}(^{235}\text{U})_{\text{tr}} \right) \\ & \left. + 2 \left( \text{moles}(^{238}\text{U})_{\text{bl}} + \text{moles}(^{238}\text{U})_{\text{tr}} \right) \right] \\ & / \left[ 5 \left( \frac{^{238}\text{U}}{^{235}\text{U}} \right)_{\text{oc}} - 2 \left( \frac{^{238}\text{U}}{^{235}\text{U}} \right)_{\text{spl}} \right] \end{aligned} \quad (36)$$

[44] The moles of  $^{238}\text{U}$  in the sample can now be determined using the  $^{238}\text{U}/^{235}\text{U}$  ratio of the sample.

$$\text{moles}(^{238}\text{U})_{\text{spl}} = \text{moles}(^{235}\text{U})_{\text{spl}} \cdot \left( \frac{^{238}\text{U}}{^{235}\text{U}} \right)_{\text{spl}} \quad (37)$$

[45] Although the solution to the system of equations in (34) and (35) yields an expression for  $\alpha_{\text{U}}$ , a simpler expression is obtained by substituting the moles of  $^{235}\text{U}$  in the sample derived in (36) into equation (34), then solving for  $\alpha_{\text{U}}$ .

$$\begin{aligned} \alpha_{\text{U}} = & \frac{1}{2} - \text{moles}(^{233}\text{U})_{\text{tr}} / \left[ 2 \left( \frac{^{233}\text{U}}{^{235}\text{U}} \right)_{\text{oc}} \cdot \left( \text{moles}(^{235}\text{U})_{\text{spl}} \right. \right. \\ & \left. \left. + \text{moles}(^{235}\text{U})_{\text{tr}} + \text{moles}(^{235}\text{U})_{\text{bl}} \right) \right] \end{aligned} \quad (38)$$

#### 2.2.4.2. Fractionation Correction and Isotope Dilution for a Single $^{235}\text{U}$ Tracer

[46] As with Pb, fractionation for a single-isotope tracer must be determined by repeated analyses of a standard. For U isotope measurements by TIMS, a single  $^{235}\text{U}$  tracer is most common, with isotopic fractionation determined by repeated analysis of CRM U500. Only the  $^{238}\text{U}/^{235}\text{U}$  ratio is measured, no oxide correction is needed, and the components of  $^{238}\text{U}$  and  $^{235}\text{U}$  are given by equation (35). Representing the sample  $^{238}\text{U}$  as the moles of  $^{235}\text{U}$  multiplied by the  $^{238}\text{U}/^{235}\text{U}$  of the sample, the resulting equation may be solved for the moles of  $^{235}\text{U}$ .

$$\begin{aligned} \text{moles}(^{235}\text{U})_{\text{spl}} = & \left[ \text{moles}(^{238}\text{U})_{\text{bl}} + \text{moles}(^{238}\text{U})_{\text{tr}} \right. \\ & \left. - \left( \frac{^{238}\text{U}}{^{235}\text{U}} \right)_{\text{meas}} (1 + 3\alpha_{\text{U}}) \left( \text{moles}(^{235}\text{U})_{\text{bl}} + \text{moles}(^{235}\text{U})_{\text{tr}} \right) \right] \\ & / \left[ \left( \frac{^{238}\text{U}}{^{235}\text{U}} \right)_{\text{meas}} (1 + 3\alpha_{\text{U}}) - \left( \frac{^{238}\text{U}}{^{235}\text{U}} \right)_{\text{spl}} \right] \end{aligned} \quad (39)$$

[47] The moles of  $^{238}\text{U}$  is calculated with equation (37).

#### 2.2.4.3. Fractionation Correction and Isotope Dilution for a Mixed $^{233}\text{U}$ - $^{236}\text{U}$ Tracer

[48] Using a mixed  $^{233}\text{U}$ - $^{236}\text{U}$  tracer, the magnitude of isotopic fractionation  $\alpha_{\text{U}}$  can be determined for each ratio measured, or on the mean of the measured ratios.

$$\alpha_{\text{U}} = \frac{1}{3} \left[ 1 - \left( \frac{^{233}\text{U}}{^{236}\text{U}} \right)_{\text{tr}} / \left( \frac{^{233}\text{U}}{^{236}\text{U}} \right)_{\text{meas}} \right] \quad (40)$$

[49] The moles of  $^{236}\text{U}$  in the tracer is equal to the concentration of  $^{236}\text{U}$  in the tracer multiplied by the measured tracer mass,

$$\text{moles}(^{236}\text{U})_{\text{tr}} = \text{conc}(^{236}\text{U})_{\text{tr}} \cdot \text{mass}_{\text{tr}} \quad (41)$$

[50] If the U is analyzed as an oxide species, then the measured  $^{238}\text{U}/^{236}\text{U}$  requires oxide correction for the isobaric interference of  $^{236}\text{U}^{18}\text{O}^{16}\text{O}$  (mass 270) on  $^{238}\text{U}^{16}\text{O}^{16}\text{O}$  (mass 270), analogous to the case presented in section 2.2.3.1 for a  $^{233}\text{U}$ - $^{235}\text{U}$  tracer. Neglecting the insignificant isobaric interference of  $^{235}\text{U}^{17}\text{O}^{16}\text{O}$  on  $^{236}\text{U}^{16}\text{O}^{16}\text{O}$  because the tracer and sample  $^{235}\text{U}$  and the  $^{17}\text{O}$  abundances are all relatively small, the oxide-corrected uranium ratios become

$$\left( \frac{^{233}\text{U}}{^{236}\text{U}} \right)_{\text{oc}} = \left( \frac{^{265}\text{UO}_2}{^{268}\text{UO}_2} \right)_{\text{meas}} \quad (42)$$

$$\left( \frac{^{238}\text{U}}{^{236}\text{U}} \right)_{\text{oc}} = \left( \frac{^{270}\text{UO}_2}{^{268}\text{UO}_2} \right)_{\text{meas}} - 2 \left( \frac{^{18}\text{O}}{^{16}\text{O}} \right) \quad (43)$$

where the result of equation (42) can be used to calculate the magnitude of isotopic fractionation in equation (40).

[51] Using the  $^{238}\text{U}/^{236}\text{U}$  measured as a metal or oxide-corrected in equation (43) and solving for the moles of  $^{238}\text{U}$  in the sample yields

$$\begin{aligned} \text{moles}(^{238}\text{U})_{\text{spl}} = & \text{moles}(^{236}\text{U})_{\text{tr}} \cdot \left[ \left( \frac{^{238}\text{U}}{^{236}\text{U}} \right)_{\text{meas}} (1 + 2\alpha_{\text{U}}) \right. \\ & \left. - \left( \frac{^{238}\text{U}}{^{236}\text{U}} \right)_{\text{tr}} \right] - \text{moles}(^{238}\text{U})_{\text{bl}} \end{aligned} \quad (44)$$

where the moles of  $^{238}\text{U}$  in the blank is calculated with equation (27).

[52] The moles of  $^{235}\text{U}$  in the sample is then determined using the  $^{238}\text{U}/^{235}\text{U}$  of the sample,

$$\text{moles}(^{235}\text{U})_{\text{spl}} = \text{moles}(^{238}\text{U})_{\text{spl}} / \left( \frac{^{238}\text{U}}{^{235}\text{U}} \right)_{\text{spl}} \quad (45)$$

### 2.2.5. Calculation of Isotopic Ratios

[53] Radiogenic isotope ratios, whose components have been corrected for fractionation and interferences as well as blank and tracer contributions, are used to calculate radiogenic isotope dates. They are also used for plotting conventional (Wetherill) and Tera-Wasserburg-type concordia diagrams.

$$\left( \frac{^{207}\text{Pb}}{^{206}\text{Pb}} \right)_{\text{rad}} = \frac{\text{moles}(^{207}\text{Pb})_{\text{rad}}}{\text{moles}(^{206}\text{Pb})_{\text{rad}}} \quad (46)$$

$$\left( \frac{^{206}\text{Pb}}{^{238}\text{U}} \right)_{\text{rad}} = \frac{\text{moles}(^{206}\text{Pb})_{\text{rad}}}{\text{moles}(^{238}\text{U})_{\text{spl}}} \quad (47)$$

$$\left( \frac{^{207}\text{Pb}}{^{235}\text{U}} \right)_{\text{rad}} = \frac{\text{moles}(^{207}\text{Pb})_{\text{rad}}}{\text{moles}(^{235}\text{U})_{\text{spl}}} \quad (48)$$

### 2.2.6. Isotopic Dates

[54] A radiogenic isotope date for either the  $^{238}\text{U}$  or  $^{235}\text{U}$  system can be derived by solving the isotopic decay equation,  $D/P = e^{-\lambda t} - 1$  for  $t$ , the time elapsed, where  $D/P$  is the present radiogenic daughter to parent ratio.

$$t_{206/238} = \frac{1}{\lambda_{238}} \log \left[ \left( \frac{^{206}\text{Pb}}{^{238}\text{U}} \right)_{\text{rad}} + 1 \right] \quad (49)$$

$$t_{207/235} = \frac{1}{\lambda_{235}} \log \left[ \left( \frac{^{207}\text{Pb}}{^{235}\text{U}} \right)_{\text{rad}} + 1 \right] \quad (50)$$

[55] To calculate a  $^{207}\text{Pb}/^{206}\text{Pb}$  date, it is not possible to solve

$$\left( \frac{^{207}\text{Pb}}{^{206}\text{Pb}} \right)_{\text{rad}} = \left( \frac{^{238}\text{U}}{^{235}\text{U}} \right)_{\text{spl}}^{-1} \cdot \frac{\exp(\lambda_{235} \cdot t_{207/206}) - 1}{\exp(\lambda_{238} \cdot t_{207/206}) - 1} \quad (51)$$

directly for  $t$ . Instead, Newton's Method, an iterative numerical solution, is used by U-Pb\_Redux.

[56] Equations to correct the isotopic dates for initial daughter isotope disequilibrium are derived in Appendix A.

### 2.2.7. Isochron Ratios and Dates

[57] Alternatively, an isochron approach uses sample isotope ratios that incorporate an initial Pbc component (equations (21) to (23)) to determine

both the isotopic date and the common Pb IC. Both two-axis plots, common in meteorite and carbonate U-Pb studies [e.g., *Patterson, 1956; Moorbath et al., 1987*], and three axis plots [*Ludwig, 1998*] that make optimum use of both U decay schemes are used.

[58] Isotopic ratios popularly used in isochron calculations include  $^{207}\text{Pb}/^{206}\text{Pb}$ ,  $^{204}\text{Pb}/^{206}\text{Pb}$ ,  $^{238}\text{U}/^{206}\text{Pb}$ ,  $^{204}\text{Pb}/^{207}\text{Pb}$ ,  $^{238}\text{U}/^{207}\text{Pb}$ ,  $^{235}\text{U}/^{207}\text{Pb}$ ,  $^{238}\text{U}/^{204}\text{Pb}$ , and  $^{235}\text{U}/^{204}\text{Pb}$ , which may be calculated using the equations for sample molar quantities above.

## 3. Uncertainty Propagation Principles

[59] In the terminology of metrology, uncertainty and error have different meanings. The uncertainty of a measured parameter refers to the dispersion of the values that could reasonably be attributed to it [*BIPM et al., 2008a*], while an error is the difference between the true (but unknown) value and the measured value.

[60] Uncertainty propagation transforms a set of several inputs, with their associated uncertainties, into the uncertainties in one or more outputs. This transformation depends upon the values and uncertainties of the inputs as well as the sensitivity of the output(s) to them. There are several algorithms that can perform this transformation, but the most popular are linear uncertainty propagation and the Monte Carlo method (MCM).

[61] Linear uncertainty propagation approximates functions in the neighborhood of their observed value by their derivative, and uses the observed values and uncertainties, assumed to be normally distributed, to find the maximum likelihood estimate of the output value. Instead of making these assumptions, the MCM uses many simulations of the uncertain value of each input to propagate their probability distribution through the data reduction equations, directly determining the expected distribution of the output. Although the MCM makes fewer assumptions, it requires  $10^5$  to  $10^6$  iterations and can thus be slow to implement for large data sets [*BIPM et al., 2008b*]. For precisely measured data, the linear approximation returns the same quality result in significantly less time, as demonstrated in section 6. U-Pb\_Redux uses this approach in order to reduce large data sets and drive interactive visualizations.

### 3.1. Determining the Uncertainties of Inputs

[62] Uncertainties in ID-TIMS measurements ultimately derive from either mass determinations with

a balance (e.g., the mass of the tracer or the masses of the isotopic reference materials used to make gravimetrically calibrated solutions) or from isotope ratio determinations made with a TIMS. For routine ID-TIMS analyses, mass determinations contribute only negligibly to the analytical uncertainty budget, and isotope ratio determinations contribute most. There are three common techniques for measuring isotope ratios with TIMS: with a static array of Faraday collectors, by a single ion counting detector such as a Daly or SEM (secondary electron multiplier), or with a combination of the two, and measurement uncertainty derives from different sources with each technique.

[63] A fixed array of Faraday collectors at unit mass spacing can be used to measure very large (>~100 pg) Pb\* samples and average-size (>~1 ng) U samples as either metal (U<sup>+</sup>) or oxide (UO<sub>2</sub><sup>+</sup>) species. Static measurements using Faraday detectors have the advantage of measuring all isotopes simultaneously. However, the amplifier circuits containing large (10<sup>11</sup> or 10<sup>12</sup> Ω) resistors that are used to measure the ion beam supply some small but constant Johnson-Nyquist (thermal) noise to each signal, in addition to the ‘shot’ noise proportional to the ion beam intensity. Each of these uncertainty contributions manifests itself in the baseline-corrected isotopic ratio measurements. For sufficiently large, stable signals, successive static Faraday isotope ratio measurements should approximate multivariate normal distributions, and their mean and uncertainty can be directly input into uncertainty propagation algorithms.

[64] The ion counter, by converting a single ion beam at a time into an electron multiplier or photomultiplier signal, is not subject to the Johnson-Nyquist noise of large resistors. However, because it is used to measure smaller (<~0.2 pA) ion beams, the signal to noise ratio is generally lower due to shot noise. Several effects specific to ion counters also contribute to the isotope ratio uncertainty, including dark noise (essentially Johnson-Nyquist noise in the electron/photomultiplier circuit) and dead time, or the inability to resolve closely spaced ion arrivals. While the dark noise can be averaged out with a sufficiently long baseline determination, the dead time must be measured and monitored closely to ensure the accuracy of ratios significantly greater or less than one (e.g., <sup>206</sup>Pb/<sup>204</sup>Pb for a radiogenic sample). Single collector measurements are subject to further uncertainty from interpolation between successive ion beam measurements as the ion beam grows and decays with time [e.g., Ludwig, 2009].

[65] In order to measure small (<0.2 pA or ~10<sup>6</sup> cps) <sup>204</sup>Pb signals on an ion counter concurrent with static measurements of <sup>205</sup>Pb to <sup>208</sup>Pb on Faraday detectors, a ‘FaraDaly’ routine is employed. The routine consists of two cycles, the first with <sup>204</sup>Pb in the ion counter and <sup>205</sup>Pb through <sup>208</sup>Pb beams in the high-mass Faraday detectors, alternating with a second cycle with <sup>205</sup>Pb in the ion counter and <sup>206</sup>Pb to <sup>208</sup>Pb beams in the Faraday detectors. The relative Faraday/ion counter gain for each cycle can be derived from the <sup>206</sup>Pb/<sup>205</sup>Pb ratio measured on the Faradays in the first cycle vs. the <sup>206</sup>Pb/<sup>205</sup>Pb ratio measured in the second cycle, with the <sup>205</sup>Pb beam on the ion counter; ratios involving <sup>204</sup>Pb from the first cycle can then be corrected for this relative gain. Because the number of measured isotope ratios to <sup>204</sup>Pb is half that of the other isotopes, conventional covariance estimation techniques (see section 3.3) are invalid, and an expectation-maximization algorithm must be employed [Dempster *et al.*, 1977].

### 3.2. Uncertainty Propagation Equation

[66] The linear uncertainty propagation equation can be derived from the Taylor series expansion of a function  $f(x)$  around the point  $x = \bar{x}$ ,

$$f(\bar{x} + \Delta x) = f(\bar{x}) + \Delta x f'(\bar{x}) + \Delta x^2 \frac{f''(\bar{x})}{2!} + \dots \quad (52)$$

the deviation of the function from its value at  $x = \bar{x}$  is expressed as the sum of the terms after  $f(\bar{x})$ , beginning with the first-order term  $\Delta x f'(\bar{x})$ . For a deviation of  $\Delta x = \sigma_x$  near  $x = \bar{x}$ , a first-order approximation of the deviation from  $y = f(x)$  is

$$\sigma_y \approx \sigma_x \frac{dy}{dx}, \quad (53)$$

where  $\frac{dy}{dx}$  is evaluated at  $x = \bar{x}$ . Squaring both sides yields the conventional linear uncertainty propagation equation for a function of a single variable, illustrated geometrically in Figure 3:

$$\sigma_y^2 \approx \sigma_x^2 \left( \frac{dy}{dx} \right)^2. \quad (54)$$

[67] The expected value of  $\Delta x^2$ , or  $(x_i - \bar{x})^2$  for a series of measurements  $x_i$  about the mean  $\bar{x}$  is the variance of  $x$ , denoted  $\sigma_x^2$ . Likewise,  $\sigma_y^2$  is the resulting square of the average deviation in  $y = f(x)$  due to the scatter in the measurements  $x_i$ . The

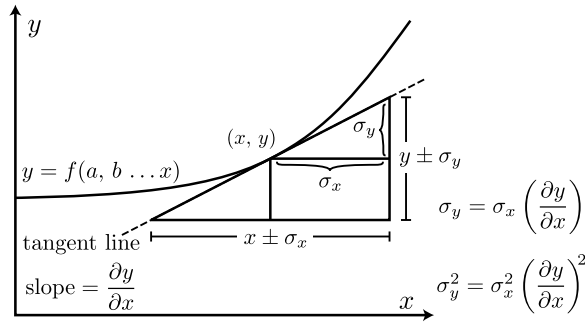


**Figure 3.** Illustration of linear uncertainty propagation for a single input parameter. Uncertainty in the  $x$  direction ( $\sigma_x$ ) of the point  $(x, y)$  results in an uncertainty  $\sigma_y$  in the function  $y = f(x)$  that is proportional to the partial derivative of  $y$  with respect to  $x$ . This estimate is accurate if the function  $f(x)$  can be approximated by its derivative at the scale of  $\sigma_x$ .

derivative is evaluated at  $x = \bar{x}$ . In dropping the higher-order terms from the Taylor series, beginning with the  $\Delta x^2$  term, this approach assumes that the uncertainty in  $x$  is relatively small compared to the curvature of  $f(x)$ , or that the function is locally linear at the scale of  $\sigma_x$  (see Figure 3).

[68] Linear uncertainty propagation for multiple inputs requires the multivariate form of the Taylor series, here expressed for two variables  $z = f(x, y)$ ,

$$f(\bar{x} + \Delta x, \bar{y} + \Delta y) = f(\bar{x}, \bar{y}) + [\Delta x f_x(\bar{x}, \bar{y}) + \Delta y f_y(\bar{x}, \bar{y})] + \frac{1}{2!} [\Delta x^2 f_{xx}(\bar{x}, \bar{y}) + 2\Delta x \Delta y f_{xy}(\bar{x}, \bar{y}) + \Delta y^2 f_{yy}(\bar{x}, \bar{y})] \dots \quad (55)$$

where  $f_x$  and  $f_{xx}$  are the first and second derivatives of  $f(x, y)$  with respect to  $x$ , respectively. The higher-order terms may again be dropped, assuming that uncertainties are small and the differentiated functions are locally linear at the scale the uncertainties of their inputs. The linear term in equation (55) again represents the deviation from the measured value  $z = f(x, y)$  encountered at a distance  $(\Delta x, \Delta y)$  from  $(\bar{x}, \bar{y})$ . Squaring the second term on the right-hand side of equation (55) yields

$$\Delta z^2 \approx \Delta x^2 f_x^2(\bar{x}, \bar{y}) + 2\Delta x \Delta y f_x(\bar{x}, \bar{y}) f_y(\bar{x}, \bar{y}) + \Delta y^2 f_y^2(\bar{x}, \bar{y})^2. \quad (56)$$

[69] Thus the expression for the variance of a function of two variables introduces a new term, the expected value of  $\Delta x \Delta y$ , or  $(x_i - \bar{x})(y_i - \bar{y})$ , which is known as the covariance between  $x$  and  $y$  and denoted  $\sigma_{xy}^2$ . Writing out the derivatives in equation (56), which are evaluated at  $(x, y) = (\bar{x}, \bar{y})$ ,

and making the above substitutions yields the conventional linear uncertainty propagation equation:

$$\sigma_z^2 = \sigma_x^2 \left( \frac{dz}{dx} \right)^2 + 2\sigma_{xy}^2 \left( \frac{dz}{dx} \right) \left( \frac{dz}{dy} \right) + \sigma_y^2 \left( \frac{dz}{dy} \right)^2. \quad (57)$$

### 3.3. Covariance and Correlation

[70] When two uncertainties are correlated, both are dependent on a common parameter or effect. One example of correlated uncertainties is between two measured isotope ratios with the same isotope in the denominator, such as the measured  $^{206}\text{Pb}/^{204}\text{Pb}$  and  $^{207}\text{Pb}/^{204}\text{Pb}$  of a radiogenic sample or between the  $^{206}\text{Pb}/^{205}\text{Pb}$  and  $^{207}\text{Pb}/^{205}\text{Pb}$  of an under-spiked sample. In the first case, the uncertainty in the measurement of the less abundant  $^{204}\text{Pb}$  denominator isotope is large, and the uncertainties of the two ratios will be highly correlated because most of the uncertainty in each isotope ratio derives from a common source, the  $^{204}\text{Pb}$  measurement. If the uncertainty in the denominator isotope is relatively small compared to those in the numerators, such as the second case above, then their uncertainties are less correlated, since most of the uncertainty in each ratio is contributed by the independent measurements of the numerator isotopes, the less abundant  $^{206}\text{Pb}$  and  $^{207}\text{Pb}$ .

[71] In both cases above, the correlation between a pair of measured isotope ratios can be determined empirically from the discrete measured data. The covariance is defined as the expected value of  $\Delta x \Delta y$ , or  $(x_i - \bar{x})(y_i - \bar{y})$  above. An unbiased estimate of the covariance,  $\sigma_{xy}^2$  can be calculated from a discrete sample of  $n$  independent measurements of  $x$  and  $y$  as

$$\sigma_{xy}^2 = \frac{1}{n-1} \sum_{i=1}^n (x_i - \bar{x})(y_i - \bar{y}) \quad (58)$$

The correlation coefficient  $\rho_{xy}$  is commonly cited because it does not depend on the magnitude of the uncertainty of  $x$  or  $y$ . It has a range of  $[-1, 1]$  inclusive and can be calculated from the covariance term above,  $\rho_{xy} = \sigma_{xy}^2 / (\sigma_x \sigma_y)$ .

[72] If discrete input data are not available, the covariance between two measured isotope ratios can be estimated using the uncertainty of a third isotope ratio that is the quotient of the first two [Schmitz and Schoene, 2007]. For instance, the covariance between the measured  $^{206}\text{Pb}/^{204}\text{Pb}$  and  $^{207}\text{Pb}/^{204}\text{Pb}$  ratios could be estimated using their uncertainties and the uncertainty in the  $^{206}\text{Pb}/^{207}\text{Pb}$  ratios from the

same data set. This approach assumes that the mean and standard error of all three ratios are calculated from the same  $n$  measurements, i.e., that no data have been discarded one ratio and not another.

[73] Other examples of variables with correlated uncertainties include isotope ratios or dates that have been subjected to a common correction, such as fractionation correction or blank and tracer subtraction. For instance, if  $x$  and  $y$  above are functions of a set of common variables  $a, b, \dots$ , then

$$\sigma_{xy}^2 = \sigma_a^2 \left( \frac{dx}{da} \right) \left( \frac{dy}{da} \right) + \sigma_b^2 \left( \frac{dx}{db} \right) \left( \frac{dy}{db} \right) + \sigma_{ab}^2 \left[ \left( \frac{dx}{da} \right) \left( \frac{dy}{db} \right) + \left( \frac{dx}{db} \right) \left( \frac{dy}{da} \right) \right] + \dots \quad (59)$$

Here,  $a, b, \dots$  could for instance be the tracer IC and enriched isotope concentrations, whose uncertainties and covariance structure,  $\sigma_a^2, \sigma_b^2, \sigma_{ab}^2, \dots$  are input by the user, and the calculated variables  $x$  and  $y$  could be the radiogenic  $^{206}\text{Pb}/^{238}\text{U}$  and  $^{207}\text{Pb}/^{235}\text{U}$  ratios. Because the variables  $x$  and  $y$  are interchangeable in equation (59), the covariance of  $x$  with  $y$  is the same as the covariance of  $y$  with  $x$ :  $\sigma_{xy}^2 = \sigma_{yx}^2$ .

[74] Equations (57) and (59) can be expanded for any number of variables and corresponding uncertainties. However, for each new variable added to equation (57), a new variance term must be added, as well as covariance terms for each new pair of variables created. The number of covariance terms grows as  $n^2$ , so that if 35 inputs and uncertainties required to reduce U-Pb data, up to 630 terms are required to completely describe their uncertainty. Furthermore, determining the total derivatives of the each output with respect to the each input through the complex series of equations presented in section 2 is a daunting task by hand, but it is required for detailed linear analysis. The covariance terms and derivatives are most easily combined for uncertainty propagation by organizing them into covariance and Jacobian matrices, respectively, and employing linear algebraic techniques.

## 4. Propagating Uncertainty With Matrices

[75] A linear algebraic framework is advantageous for uncertainty propagation because it efficiently organizes the covariance and derivative terms presented above into matrices. Matrix multiplication is computationally fast, which enables rapid updates as the analyst explores parameter space in the graphical user interface of U-Pb\_Redux. Derivatives of the

intermediate reduction parameters and outputs calculated in equations (2) to (51) can be organized into Jacobian matrices (section 4.1) according to simple rules, a process that can be automated with software [Bowring *et al.*, 2011], ensuring accuracy in what would be many complex equations expressed longhand. The variance and covariance structure of the input variables are arranged in a single covariance matrix (section 4.1), and all other correlation determinations are the product of straightforward matrix multiplication, so there is no propagation of uncertainty through multiple intermediate formulations. In this way, matrix representation ensures that covariance terms are carried through the entire uncertainty propagation calculation, and terms that may become important in the future are never ignored for simplicity. Finally, covariance and Jacobian matrices can be formulated with a block structure if analytical, tracer, and/or decay constant uncertainties are considered independent, so that matrix multiplication is broken down into small, quickly calculated pieces.

### 4.1. Covariance and Jacobian Matrices

[76] Uncertainty propagation using matrix multiplication utilizes two types of matrices, covariance matrices and Jacobian matrices. A covariance matrix describes the uncertainties of a set of variables and how they relate to one another. For  $n$  variables, it takes the form

$$\Sigma = \begin{bmatrix} \sigma_1^2 & \sigma_{12}^2 & \dots & \sigma_{1n}^2 \\ \sigma_{12}^2 & \sigma_2^2 & \dots & \sigma_{2n}^2 \\ \vdots & \vdots & \ddots & \vdots \\ \sigma_{1n}^2 & \sigma_{2n}^2 & \dots & \sigma_n^2 \end{bmatrix}$$

Matrix elements in the first row and first column of the covariance matrix relate to the first variable, elements in the second row or second column to the second variable, and so on. Terms on the diagonal of the covariance matrix (e.g.,  $\sigma_1^2$  and  $\sigma_2^2$ ) are variances; the off-diagonal elements are covariance terms. For instance, the matrix element in the first row and second column is the covariance between the first and second variable,  $\sigma_{12}^2$ . The covariance matrix is symmetric because  $\sigma_{12}^2 = \sigma_{21}^2$ . Independent, uncorrelated variables have zero covariance.

[77] The other component of linear algebraic uncertainty propagation, a Jacobian matrix, describes a linear transformation from the input parameters to the output variables. In the context of uncertainty

propagation, the Jacobian matrix approximates the sensitivity of output variables to small changes in their input parameters as the partial derivative of the function of the output with respect to each input. For a set of  $m$  functions  $f_1$  to  $f_m$  of  $n$  variables  $x_1$  to  $x_n$ , a Jacobian matrix takes the form

$$J_1 = \begin{bmatrix} \frac{\partial f_1}{\partial x_1} & \frac{\partial f_1}{\partial x_2} & \cdots & \frac{\partial f_1}{\partial x_n} \\ \frac{\partial f_2}{\partial x_1} & \frac{\partial f_2}{\partial x_2} & \cdots & \frac{\partial f_2}{\partial x_n} \\ \vdots & \vdots & \ddots & \vdots \\ \frac{\partial f_m}{\partial x_1} & \frac{\partial f_m}{\partial x_2} & \cdots & \frac{\partial f_m}{\partial x_n} \end{bmatrix}$$

Each row of the Jacobian corresponds to an input variable,  $x_1, x_2, \dots$  and each column an output,  $f_1(x_1, x_2, \dots), f_2(x_1, x_2, \dots)$ . Every entry in the matrix is the partial derivative of the column variable with respect to the row variable. If the function  $f_i$  is not defined in terms of the input  $x_j$ , then the value of the partial derivative  $\partial f_i / \partial x_j$  is zero. These derivatives may be calculated after analytical differentiation [e.g., Schmitz and Schoene, 2007; Bowring et al., 2011] or approximated numerically [e.g., Roddick, 1987; Scaillet, 2000].

[78] The data reduction equations (1) to (51) in section 2 do not express the output variables (e.g., the  $^{206}\text{Pb}/^{238}\text{U}$  date) as a lengthy single function of the input parameters (e.g., the measured  $^{206}\text{Pb}/^{205}\text{Pb}$ ). The output isotopic dates and ratios are instead most straightforwardly written in terms of a series of intermediate parameters (e.g., moles ( $^{206}\text{Pb}$ )<sub>bl</sub>), which accomplish the calculation in several steps. However, the uncertainty propagation algorithm presented in equation (57) requires the partial derivatives of the output  $z$  with respect to the inputs  $x$  and  $y$ .

## 4.2. Calculating the Total Derivative

[79] Because the output isotopic dates and ratios are not defined directly as a function of the input parameters, their partial derivatives are not defined as well. When several intermediate steps precede a final output, its total derivative is required for uncertainty propagation, which incorporates each way the output is contingent upon the input. For instance, the  $^{207}\text{Pb}/^{206}\text{Pb}$  date depends on the measured  $^{204}\text{Pb}/^{205}\text{Pb}$  in two ways. The measured  $^{204}\text{Pb}/^{205}\text{Pb}$  is first fractionation corrected in equation (3), then used to calculate both the moles of  $^{206}\text{Pb}$  and of  $^{207}\text{Pb}$  in the laboratory blank in equations (15) and (16). The moles of blank of both

isotopes are subsequently subtracted from the measured moles  $^{206}\text{Pb}$  and  $^{207}\text{Pb}$  in equations (18) and (19) to determine the radiogenic  $^{207}\text{Pb}/^{206}\text{Pb}$  ratio (equation (46)) and the  $^{207}\text{Pb}/^{206}\text{Pb}$  date (equation (51)). Thus the uncertainty in the  $^{207}\text{Pb}/^{206}\text{Pb}$  date receives two contributions from the  $^{204}\text{Pb}/^{205}\text{Pb}$  uncertainty: from the moles  $^{206}\text{Pb}$  and  $^{207}\text{Pb}$ . Both contributions are included in the total derivative.

[80] In a linear algebraic framework, total derivatives are calculated by multiplying two or more Jacobian matrices. The rightmost matrix in the matrix product contains partial derivatives of the first set of intermediate parameters with respect to the inputs that define them. For instance, the first Jacobian matrix could contain the moles of  $^{205}\text{Pb}$  in the tracer (equation (1)) and the fractionation-corrected  $^{204}\text{Pb}/^{205}\text{Pb}$  ratio (equation (3)), which are both defined in terms of input parameters. If this matrix is left-multiplied by another Jacobian matrix containing the partial derivatives of the moles of  $^{206}\text{Pb}$  and  $^{207}\text{Pb}$  in the blank (equations (15) and (16)) with respect to the moles of  $^{205}\text{Pb}$  in the tracer and the fractionation-corrected  $^{204}\text{Pb}/^{205}\text{Pb}$  ratio, the product will include the total derivative of the moles of  $^{206}\text{Pb}$  and  $^{207}\text{Pb}$  in the blank with respect to the input parameters.

[81] If  $f_1$  and  $f_2$  are functions of the input parameters  $x_1$  and  $x_2$ , and  $g_1$  and  $g_2$  are in turn functions of  $f_1$  and  $f_2$ , then the total derivative of the functions  $g_1$  and  $g_2$  with respect to  $x_1$  and  $x_2$  is the product of two Jacobian matrices,  $J_1$  and  $J_2$

$$\begin{bmatrix} \frac{dg_1}{dx_1} & \frac{dg_2}{dx_1} \\ \frac{dg_1}{dx_2} & \frac{dg_2}{dx_2} \end{bmatrix} = \begin{bmatrix} \frac{\partial f_1}{\partial x_1} & \frac{\partial f_2}{\partial x_1} \\ \frac{\partial f_1}{\partial x_2} & \frac{\partial f_2}{\partial x_2} \end{bmatrix} \begin{bmatrix} \frac{\partial g_1}{\partial f_1} & \frac{\partial g_2}{\partial f_1} \\ \frac{\partial g_1}{\partial f_2} & \frac{\partial g_2}{\partial f_2} \end{bmatrix} \quad (60)$$

or  $J = J_1 J_2$

The first column of the matrix product  $J$  is the total derivative of the output function  $g_1$  with respect to each of the input variables  $x_1$  and  $x_2$ ; the second column contains the derivatives of  $g_2$ . Expanding the matrix multiplication for the element in the first row and column of  $J$  reveals

$$\frac{dg_1}{dx_1} = \frac{\partial g_1}{\partial f_1} \frac{\partial f_1}{\partial x_1} + \frac{\partial g_1}{\partial f_2} \frac{\partial f_2}{\partial x_1} \quad (61)$$

which is the equation for the total derivative of  $g_1$  with respect to  $x_1$ .

[82] To propagate uncertainties for a more complex system, matrix  $J_1$  of equation (60) can be modified

so that it contains rows for  $n$  input parameters ( $x_1, x_2, \dots, x_n$ ) and columns for  $m$  intermediate parameters ( $f_1, f_2, \dots, f_m$ ), where those parameters are expressed as functions of the input parameters. Matrix  $J_2$  must be adjusted as well to contain  $m$  rows for the intermediate parameters in  $J_1$ , with  $p$  columns for the next set of intermediate parameters  $g_1, g_2, \dots, g_p$ . Further Jacobian matrices  $J_3, J_4, \dots$  can be added until the final set of output parameters has been reached.

[83] This technique is utilized in U-Pb\_Redux. The partial derivatives of the data reduction equations in section 2 and Appendix A are calculated during data reduction. These are arranged into approximately ten Jacobian matrices, depending on the tracer and common Pb correction scheme employed, that start with the input variables, step through the intermediate variables, and end with the output isotope ratios and dates. The product is the Jacobian matrix  $J$ , a linearized model of the data reduction equations that contains the total derivatives of the isotopic dates and ratios in sections 2.2.5 and 2.2.6 and Appendix A with respect to the user-input parameters in Tables 1 and 2.

### 4.3. Uncertainty Propagation Equation

[84] Using the covariance and Jacobian matrices assembled above, the uncertainty propagation equation for  $z = f(x, y)$  (equation (57)), can be restated as a matrix product,

$$\sigma_z^2 = \begin{bmatrix} \frac{dz}{dx} & \frac{dz}{dy} \end{bmatrix} \begin{bmatrix} \sigma_x^2 & \sigma_{xy}^2 \\ \sigma_{xy}^2 & \sigma_y^2 \end{bmatrix} \begin{bmatrix} \frac{dz}{dx} \\ \frac{dz}{dy} \end{bmatrix} = J^T \Sigma J \quad (62)$$

To calculate the uncertainty and covariance between multiple outputs, the outermost Jacobian matrix contains a column for each output. The matrix product then yields the covariance matrix of the output parameters. For example, if  $w$  is also a function of  $x$  and  $y$ , then by calculating the product

$$\begin{bmatrix} \sigma_z^2 & \sigma_{zw}^2 \\ \sigma_{zw}^2 & \sigma_w^2 \end{bmatrix} = \begin{bmatrix} \frac{dz}{dx} & \frac{dw}{dx} \\ \frac{dz}{dy} & \frac{dw}{dy} \end{bmatrix}^T \begin{bmatrix} \sigma_x^2 & \sigma_{xy}^2 \\ \sigma_{xy}^2 & \sigma_y^2 \end{bmatrix} \begin{bmatrix} \frac{dz}{dx} & \frac{dw}{dx} \\ \frac{dz}{dy} & \frac{dw}{dy} \end{bmatrix} \quad (63)$$

the uncertainty in  $w$ ,  $\sigma_w^2$  and the covariance between  $z$  and  $w$ ,  $\sigma_{zw}^2$  fall out.

[85] The covariance matrix  $\Sigma$  can be expanded for any number of inputs, and the Jacobian matrix  $J$  can represent the product of several intermediate Jacobian matrices  $J_1, J_2, \dots$ . In this way, uncertainty

propagation for a complex system of inputs, intermediate parameters, and related outputs is represented by a single matrix equation. Because  $J$  contains the total derivatives of the outputs with respect to the inputs, covariance terms do not need to be calculated in uncertainty propagation expressions for every intermediate parameter. The intermediate parameters can now be defined as parameters of interest instead of being formulated to facilitate covariance calculations. An illustration of the U-Pb uncertainty propagation algorithm with populated covariance and Jacobian matrices can be found in the auxiliary material.<sup>1</sup>

## 5. Weighted Means

[86] The goal of calculating a weighted mean is to report a single date and uncertainty that best represents the knowledge accumulated by a set of measurements that are assumed to represent a single population with normally distributed uncertainties. Every weighted mean algorithm involves assigning weights, or multipliers which sum to unity, to the measurements, then summing the weighted data. The arithmetic mean gives each of  $n$  measurements an equal weight of  $1/n$ , but a weighted mean may assign a unique weight to each datum so that precise data are weighted more heavily.

### 5.1. Conventional Weighted Mean of Independent Data

[87] For the weighted mean  $\bar{t}$  of  $n$  independent measurements  $t_1, \dots, t_n$ , the weights  $\alpha_1, \dots, \alpha_n$  are inversely proportional to the variance of each date,  $\sigma_1^2, \dots, \sigma_n^2$ , so that

$$\alpha_i = \frac{1}{\sigma_i^2} / \sum_{i=1}^n \left( \frac{1}{\sigma_i^2} \right)$$

where the denominator is used to normalize the sum of the weights. Thus the weighted mean  $\bar{t}$  is

$$\bar{t} = \sum_{i=1}^n \alpha_i t_i = \sum_{i=1}^n \left( \frac{t_i}{\sigma_i^2} \right) / \sum_{i=1}^n \left( \frac{1}{\sigma_i^2} \right) \quad (64)$$

This choice of weights minimizes the sum of the squared difference between each date and the mean, divided by the date's variance,

$$S = \sum_{i=1}^n \frac{(t_i - \bar{t})^2}{\sigma_i^2} \quad (65)$$

<sup>1</sup>Auxiliary materials are available in the HTML. doi:10.1029/2010GC003478.

The statistic  $S$  has a  $\chi^2$  distribution with  $n - 1$  degrees of freedom. The quotient  $S/(n - 1)$  is the ‘mean square of weighted deviates’ (MSWD) [e.g., *Wendt and Carl, 1991*], which characterizes the goodness of fit, or how well the weighted mean  $\bar{t}$  describes the data  $t_i$ . MSWD values close to one indicate that the scatter in the data  $t_i$  can be explained by their uncertainties  $\sigma_i$ . Values much lower or greater than one may indicate that the uncertainties have been overestimated or underestimated, respectively. Minimizing  $S$ , which also minimizes the MSWD and the uncertainty of  $\bar{t}$ , concurrently maximizes the likelihood that, given the measurements  $t_1, \dots, t_n$ , the mean is  $\bar{t}$ .

[88] The uncertainty of  $\bar{t}$  can be derived using the conventional uncertainty propagation equation. The derivative of  $\bar{t}$  with respect to a date,  $t_i$  in equation (64) is

$$\frac{\partial \bar{t}}{\partial t_i} = \frac{1}{\sigma_i^2} / \sum_{i=1}^n \left( \frac{1}{\sigma_i^2} \right) = \alpha_i$$

Assuming that the dates  $t_1, \dots, t_n$  have uncorrelated uncertainties, the variance of  $\bar{t}$ , according to the uncertainty propagation equation (57) is

$$\sigma_{\bar{t}}^2 = \sum_{i=1}^n \left[ \left( \frac{\partial \bar{t}}{\partial t_i} \right)^2 \cdot \sigma_i^2 \right] = \sum_{i=1}^n \left[ \left( \frac{1}{\sigma_i^2} \right)^2 / \left( \sum_{i=1}^n \left( \frac{1}{\sigma_i^2} \right) \right)^2 \cdot \sigma_i^2 \right]$$

Combining numerator terms and factoring out a common denominator yields,

$$\sigma_{\bar{t}}^2 = \sum_{i=1}^n \left[ \sigma_i^2 \left( \frac{1}{\sigma_i^2} \right)^2 \right] / \left( \sum_{i=1}^n \left( \frac{1}{\sigma_i^2} \right) \right)^2$$

Finally, dividing out a  $\sigma_i^2$  term in the numerator gives the form  $x/x^2$ , which simplifies to

$$\sigma_{\bar{t}}^2 = 1 / \sum_{i=1}^n \left( \frac{1}{\sigma_i^2} \right). \quad (66)$$

[89] Equations (64) and (66) assume, however, that each of the measured dates  $t_i$  are independent: that none of their uncertainties share a common systematic contribution. Although these equations can be used to propagate random analytical uncertainties, they cannot assess the systematic contribution of tracer or decay constant uncertainties to a weighted mean date. In the past, systematic errors have been added in quadrature after equations (64) and (66) are evaluated with analytical uncertainties.

However, this approach cannot accurately handle several important scenarios.

[90] First, if a systematic variable affects each analysis differently, it is unclear which magnitude to add in quadrature. One example is combining analyses with different ratios of tracer to sample. Because the magnitude of the tracer subtraction is different for each, the uncertainty contribution from the subtraction is also different. Also, because the estimated IC of the tracer differs from the true value (within uncertainty), tracer subtraction will introduce some scatter in the results. If the estimated tracer  $^{206}\text{Pb}/^{205}\text{Pb}$  ratio is greater than, but within uncertainty of, the true  $^{206}\text{Pb}/^{205}\text{Pb}$  ratio, then the moles of radiogenic  $^{206}\text{Pb}$  in under-spiked analyses will be overcorrected for the  $^{206}\text{Pb}$  in the tracer in equation (18), and overspiked analyses will be overcorrected even further. This scatter, which is introduced by a systematic source, must be considered along with the scatter from random effects during calculation of weighted mean statistics, so that it is not interpreted as ‘geologic scatter.’

[91] Second, it is unclear how to propagate uncertainty which has both a random component and a systematic component with equations (64) and (66). For instance, correction for Pb fractionation using a single-isotope Pb tracer is usually performed by repeatedly analyzing a certified reference material, e.g., NBS981. The random uncertainty propagated in the fractionation correction is often taken as the long-term reproducibility of this standard, but the uncertainty also contains a systematic component related to the uncertainty in the certified IC of NBS981. The latter cannot be reduced by repeated analyses, which would occur if this uncertainty were considered as analytical and included in  $\sigma_i$  in equation (66).

[92] The solution to both of the scenarios above is to treat systematic uncertainties as uncertainty correlations between analyses, yielding a weighted mean, its uncertainty, and an MSWD that is not artificially deflated by misattributed uncertainties.

## 5.2. The Date Covariance Matrix

[93] As section 3.3 details, correlations arise between calculated values when they rely on common parameters. In the case of weighted mean U-Pb dates, two large uncertainty contributions from common parameters are the IC and U/Pb ratio of the tracer, and the decay constant uncertainties. The covariance matrix for a measured data set of isotopic dates can be constructed with each date’s variance ( $1\sigma$



uncertainty, squared) on its diagonal. The variance includes uncertainty contributions from both random and systematic effects. Off-diagonal elements characterize the correlation between pairs of dates. Along with the numerical dates themselves, the date covariance matrix,  $\Sigma$ , can then be used to calculate a generalized weighted mean [Lyons *et al.*, 1988; Valassi, 2003] that accounts for both random and systematic uncertainties.

[94] The date covariance matrix can be calculated using the linear algebraic methods presented in section 4.3. The total derivative of each date with respect to each common variable is calculated when multiplying Jacobian matrices during the uncertainty propagation for each fraction (section 4). For instance in equation (60), the total derivatives for the output variable  $g_1$  with respect to the inputs  $x_1, x_2$  are found in the first column and first two rows of matrix  $J$ .

[95] Analogously, each column of the product of the Jacobian matrices of the U-Pb uncertainty propagation equations contains the derivatives of the one of the outputs, for instance the  $^{206}\text{Pb}/^{238}\text{U}$  date. Several rows in this column contain the derivatives with respect to variables shared with the other dates, such as the tracer parameters and the decay constants. The  $m$  rows corresponding to the systematically varying uncertainties in the column corresponding to the  $^{206}\text{Pb}/^{238}\text{U}$  date can be extracted from the Jacobian matrix for each of the  $n$  fractions to be averaged. The resulting columns are appended to create a new  $m$  by  $n$  Jacobian matrix,  $J_t$ . Each column of the new matrix corresponds to the  $^{206}\text{Pb}/^{238}\text{U}$  date of the  $n$  fractions, and each row corresponds to one of the  $m$  systematically varying parameters.

[96] Using  $J_t$  and the input covariance matrix for the set of common variables, the systematic covariance matrix  $\Sigma_{ts}$  for the dates can be calculated using equation (62),

$$\Sigma_{ts} = J_t^T \Sigma_s J_t \quad (67)$$

where  $\Sigma_s$  is the  $m$  by  $m$  covariance matrix of the systematic uncertainties to be propagated and  $\Sigma_{ts}$  is the  $n$  by  $n$  covariance matrix describing the systematic uncertainty contributions to the  $n$  dates. Another  $n$  by  $n$  covariance matrix  $\Sigma_{tr}$  describes the random (analytical) uncertainties for each date, with the analytical variance for each date on its diagonal. The covariance matrix  $\Sigma$  for the dates is then the sum of the random and systematic components of uncertainty,

$$\Sigma = \Sigma_{ts} + \Sigma_{tr} \quad (68)$$

### 5.3. Generalized Weighted Mean of Correlated Data

[97] The derivation for a generalized weighted mean of correlated measurements is analogous to the derivation for the conventional weighted mean above. Following Lyons *et al.* [1988], the best linear unbiased estimate (BLUE) of the generalized weighted mean,  $\hat{t}$ , given the correlated measurements  $t_1, \dots, t_n$  is a weighted linear sum of the data that simultaneously minimizes the uncertainty of the estimate  $\hat{t}$  and the MSWD, maximizing the probability that  $\hat{t}$  is the mean of the data. The generalized weighted mean can be represented by a sum of scalar products as in equation (64), or equivalently as the dot product of two vectors, hereafter displayed in bold, containing the weights and the observed data

$$\hat{t} = \sum_{i=1}^n \alpha_i t_i = \alpha^T \mathbf{t} \quad (69)$$

[98] Unlike the conventional weighted mean, there is no simple formula for the generalized weighted mean weights. Instead, the vector of weights,  $\alpha$ , is determined using the fact that it minimizes the uncertainty in  $\hat{t}$ . Analogous to the ‘conventional’ weighted mean derivation, the derivative of  $\hat{t}$  with respect to the vector of measured dates  $\mathbf{t}$  is

$$\partial \hat{t} / \partial \mathbf{t} = \alpha$$

The resulting vector of derivatives is the Jacobian matrix of the function  $\hat{t}$ . Along with the covariance matrix for the measured dates derived in section 5.2, the Jacobian matrix can be substituted into equation (62), the linear algebraic uncertainty propagation equation, to yield,

$$\sigma_{\hat{t}}^2 = \alpha^T \Sigma \alpha \quad (70)$$

where  $\Sigma$  is the covariance matrix of the dates. Minimizing  $\sigma_{\hat{t}}^2$  subject to the constraint that the sum of the weights in  $\alpha$  is unity is most easily accomplished with a Lagrange multiplier.

[99] A common strategy for solving constrained minimization problems, a Lagrange multiplier is introduced to find the extrema of the function  $f(\alpha)$  subject to the constraint  $g(\alpha) = c$ . Here,  $f(\alpha)$  is equation (70) and the constraint that the sum of the weights equal unity can be restated as a vector product,  $\alpha^T \mathbf{1} = 1$ , where  $\mathbf{1}$  is a  $n$ -component column vector of ones. At an extremum of  $f(\alpha)$ , the gradients

of  $f(\alpha)$  and  $g(\alpha)$  are parallel, although not necessarily the same magnitude. Thus,

$$\nabla f(\alpha) = -\lambda \nabla g(\alpha)$$

and  $\lambda$  is known as the Lagrange multiplier. Utilizing the linearity of the gradient operator, such that  $\nabla F + \nabla g = \nabla(f + g)$ , both terms can be moved to the left-hand side of the equation and combined. Enforcing the constraint that  $g(\alpha) = c$  gives

$$\nabla[f(\alpha) + \lambda \cdot (g(\alpha) - c)] = \mathbf{0}$$

where  $\mathbf{0}$  is a matrix of zeros. Substituting the generalized weighted mean equation and constraints yields the gradient of a function  $F$ ,

$$\nabla F = \nabla[\alpha^T \Sigma \alpha + \lambda \cdot (\alpha^T \mathbf{1} - 1)] = \mathbf{0}$$

[100] The gradient may be decomposed into the partial derivatives with respect to the two variables,  $\alpha$  and  $\lambda$ , which both evaluate to zero. Because the covariance matrix  $\Sigma$  is symmetric,  $\Sigma^T = \Sigma$ , producing two equations,

$$\frac{\partial F}{\partial \alpha} = (\Sigma^T + \Sigma)\alpha + \lambda \mathbf{1} = 2\Sigma\alpha + \lambda \mathbf{1} = \mathbf{0} \quad (71)$$

$$\frac{\partial F}{\partial \lambda} = \alpha^T \mathbf{1} - 1 = 0 \quad (72)$$

with two unknowns,  $\lambda$  and  $\alpha$ .

[101] A solution to this system of equations is found by first solving equation (71) for  $\alpha$ , then substituting this expression into equation (72) and evaluating the transpose,

$$\alpha = -\frac{1}{2} \lambda \Sigma^{-1} \mathbf{1}$$

$$-\left(\frac{1}{2} \lambda \Sigma^{-1} \mathbf{1}\right)^T \mathbf{1} = -\frac{1}{2} \lambda \mathbf{1}^T \Sigma^{-1} \mathbf{1} = 1$$

Where  $\Sigma^{-1}$  is the inverse of the date covariance matrix. Because  $\mathbf{1}^T \Sigma^{-1} \mathbf{1}$  is a scalar quantity, it can be moved to the denominator. The resulting equation can be solved for  $\lambda$  and substituted back into equation (71), yielding

$$\lambda = -2 / (\mathbf{1}^T \Sigma^{-1} \mathbf{1})$$

$$2\Sigma\alpha + \left[-2 / (\mathbf{1}^T \Sigma^{-1} \mathbf{1})\right] \mathbf{1} = \mathbf{0}$$

Finally, solving for  $\alpha$  gives

$$\alpha = \Sigma^{-1} \mathbf{1} / (\mathbf{1}^T \Sigma^{-1} \mathbf{1}) \quad (73)$$

[102] To evaluate the generalized weighted mean, the expression for  $\alpha$  in equation (73) can be substituted into equation (69), producing the equation for the generalized weighed mean,

$$\hat{t} = \mathbf{1}^T \Sigma^{-1} \mathbf{t} / (\mathbf{1}^T \Sigma^{-1} \mathbf{1}) \quad (74)$$

The expression for  $\alpha$  in equation (73) can also be substituted into equation (70), yielding

$$\sigma_i^2 = (\Sigma^{-1} \mathbf{1})^T \Sigma (\Sigma^{-1} \mathbf{1}) / (\mathbf{1}^T \Sigma^{-1} \mathbf{1})^2$$

Evaluating the transpose and canceling terms in the numerator yields the form  $x/x^2$ , which simplifies to

$$\sigma_i^2 = 1 / (\mathbf{1}^T \Sigma^{-1} \mathbf{1}) \quad (75)$$

The variance of the generalized weighed mean is thus equal to the reciprocal of the sum of the terms in the inverse covariance matrix  $\Sigma^{-1}$ . For the special case when the uncertainties in all dates are independent,  $\Sigma$  and thus  $\Sigma^{-1}$  become diagonal matrices and equation (75) evaluates to equation (66).

[103] Analogous to equation (65), the goodness of fit, or degree to which the weighted mean  $\hat{t}$  fits the observed data  $t_i$ , is described by the statistic

$$S = \mathbf{r}^T \Sigma^{-1} \mathbf{r} \quad (76)$$

where  $\mathbf{r}$  is the vector of residuals  $r_i = t_i - \hat{t}$ .  $S$  has a  $\chi^2$  distribution with  $n - 1$  degrees of freedom, and dividing  $S$  by  $n - 1$  yields the familiar MSWD.

## 5.4. Application to U-Pb Geochronology

[104] For U-Pb geochronology by ID-TIMS, the largest systematic uncertainty contributions come from the tracer IC and enriched isotope concentrations and from the uncertainty in the decay constants. While analytical uncertainties alone are used to compare U-Pb analyses measured with the same tracer, it is necessary to propagate the tracer uncertainties in order to compare with U-Pb analyses measured with a different tracer. Comparison of U-Pb dates with other decay systems, such as  $^{40}\text{Ar}$ - $^{39}\text{Ar}$ , requires propagating the U decay constant uncertainties as well. These three uncertainties are often represented in the form  $\pm X/Y/Z$ , where  $X$  is the analytical uncertainty,  $Y$  includes the analytical and tracer contributions, and  $Z$  includes the analytical, tracer and decay constant uncertainties [e.g., *Schoene and Bowring, 2006*].

[105] The generalized weighted mean algorithm is used by U-Pb\_Redux to calculate  $X$ ,  $Y$ , and  $Z$ . The covariance matrix  $\Sigma_{tr}$  of random uncertainties is first assembled by placing the analytical uncertainties for each of  $n$  dates along the diagonal of an  $n$  by  $n$  matrix  $\Sigma_{tr}$ . Evaluating equations (73) to (76) with  $\Sigma = \Sigma_{tr}$  is mathematically equivalent to using equations (64) to (66) for independent measurements, and gives the uncertainty  $X$ .

[106] Following section 5.2, covariance matrices for the dates which contain the tracer and decay constant uncertainties are assembled using equation (67). To calculate  $Y$ , only the tracer parameter uncertainties are included in  $\Sigma_{ts}$ , and to calculate  $Z$ , both the tracer and decay constant uncertainties are present. The matrix  $\Sigma_{ts}$  for the tracer and decay constants also contains elements for any covariance between the two, which would be incurred if for instance the  $^{235}\text{U}$  decay constant were recalibrated to the  $^{238}\text{U}$  decay constant using closed system zircon analyses spiked with the same tracer [Schoene et al., 2006; Mattinson, 2010].

[107] The MSWD calculated using equation (76) for the generalized weighted mean is different for  $X$ ,  $Y$ , and  $Z$ . We recommend using the MSWD calculated for  $Z$  because it accurately incorporates all sources of scatter.

## 6. Verification by Monte Carlo Method

[108] The linear uncertainty propagation equations presented above are based upon several important assumptions. First, in order to interpret output covariance matrices in terms of confidence intervals, for example that  $\pm 2\sigma$  approximates a 95% confidence interval (CI) about an isotopic date, the uncertainties of the inputs are all assumed to have normal (Gaussian) probability distributions. This assumption is typically justified using the central limit theorem, which states that the mean of many small random effects is approximately normally distributed, even if the probability distribution of the effects are not.

[109] Most, if not all, uncertainties for ID-TIMS measurements are observed to be normally distributed. The isotope measurements in the numerator and denominator of isotope ratios are assumed to be controlled by Poisson processes, which yield asymmetric Poisson probability distributions for low count rates. However, at the count rates (generally  $>10$  cps) and integration times (generally  $>100$  s total) usually used for U-Pb geochronology by ID-TIMS, these distributions can be closely approximated as Gaussian.

In addition, the uncertainties in isotope ratios also contain contributions from other sources, such as resistor noise and beam interpolation. Although a Student's  $t$ -distribution is appropriate for discrete data with finite degrees of freedom, U-Pb analyses typically contain  $>50$  ratio measurements, at which point the Student's  $t$  and the normal distributions are almost identical.

[110] Other input uncertainties, such as isotopic fractionation or the blank isotopic composition, can often be measured with higher precision than their external variability. For instance, the variability in the Pb blank IC is most likely due to variable magnitude contributions from various Pb contamination sources, such as ion exchange chemistry and sample loading. The average effect of these small variations, as predicted by the central limit theorem, is an observed normal distribution. This reasoning is also extended to unobservable quantities, such as the Th/U ratio of the magma used for  $^{230}\text{Th}$ -correction of  $^{206}\text{Pb}/^{238}\text{U}$  dates [e.g., Crowley et al., 2007].

[111] Another assumption made by linear uncertainty propagation, illustrated in Figure 3, is that the magnitude of the input uncertainties are small, so that the function  $y = f(x)$  is locally linear at the scale of  $\sigma_x$ . This is equivalent to the assumption that the higher-order terms in the Taylor series in equation (55) are insignificant. Because the data reduction equations are not linear (they involve division, exponentiation, and logarithms) this assumption depends upon the magnitude of the observed input uncertainties. To test whether linear uncertainty propagation algorithm implemented in U-Pb\_Redux accurately models the uncertainty of isotopic dates with typical ID-TIMS input uncertainties, the Monte Carlo method (MCM) is used.

### 6.1. Monte Carlo Experimental Setup

[112] Implementation of MCM begins by specifying a probability distribution for each input variable [BIPM et al., 2008b; Cox and Siebert, 2006]. For this implementation, all input variables are assumed to have multivariate normal probability distributions, but MCM can also be implemented with other (e.g., uniform) input distributions. Next, a pseudo-random number generator is used to produce a random sample, known as a Monte Carlo trial, from the input probability distribution for each parameter. These values are used to calculate the output variables, e.g., isotopic dates, and then the process is repeated  $M$  times. The resulting distribution of the  $M$  values for an output approximates its probability distribution, and if several outputs are calculated

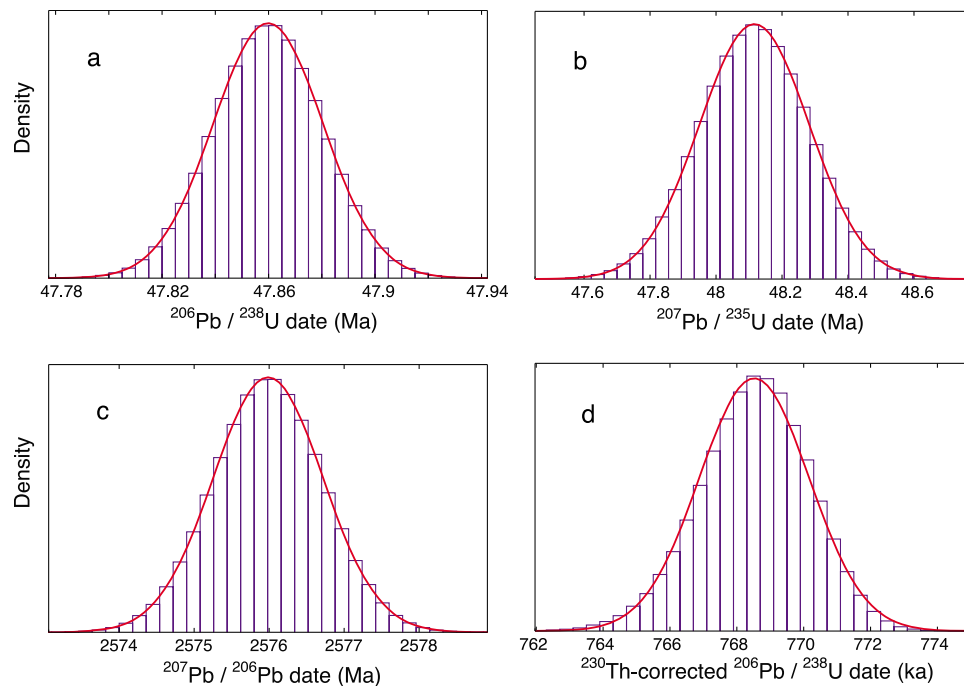


**Figure 4.** Histograms illustrating the results of  $10^6$  Monte Carlo simulations for three representative ID-TIMS zircon analyses. Red curves are normal distributions corresponding to the date and uncertainty calculated by U-Pb\_Redux. (a) Monte Carlo simulations of the  $^{206}\text{Pb}/^{238}\text{U}$  date of an Eocene zircon, (b) the  $^{207}\text{Pb}/^{235}\text{U}$  date of the same analysis, and (c) the  $^{207}\text{Pb}/^{206}\text{Pb}$  date of an Archean zircon are normally distributed, with the same mean and uncertainty calculated by U-Pb\_Redux. The distribution of Monte Carlo trials for a young (d) Th-corrected Bishop Tuff grain is slightly right skewed but can be closely approximated by its linear uncertainty propagation result.

from the same input trials, the result approximates their joint probability distribution, which describes their correlation as well.

[113] There are multiple ways to interpret the output of a Monte Carlo model. If the  $M$  calculated output variables are normally distributed, then two standard deviations about the mean is a good estimate of the 95% CI. When the results are not normally distributed, then multiple 95% CIs can be reported. The two most popular are the 95% CI that is symmetric about the mean of the distribution and the shortest 95% CI [BIPM *et al.*, 2008b]. For probability distributions close to normal, the form of the first is most familiar and is used here.

## 6.2. Results

[114] The MCM has been utilized before for U-Pb data [Briqueu and de la Boisse, 1990], but never in the context of calculating radiogenic U-Pb dates from measured data or testing a U-Pb uncertainty propagation algorithm. Here we present data for three ID-TIMS zircon analyses with typical analytical uncertainties. The mathematical programming environment MATLAB was used to generate

$M = 10^6$  multivariate normal Monte Carlo trials from the measured and estimated input parameters and uncertainties. The results of Monte Carlo method modeling are plotted as histograms and best-fit normal distributions and presented in Figure 4.

[115] The first analysis modeled by MCM is an Eocene zircon with a Pb\*/Pbc, or ratio of total radiogenic to common Pb, of  $\sim 18$ . The measured  $^{206}\text{Pb}/^{205}\text{Pb}$  and  $^{207}\text{Pb}/^{205}\text{Pb}$  uncertainties are 0.025% and 0.090%, respectively. U-Pb\_Redux calculates a  $^{206}\text{Pb}/^{238}\text{U}$  date of  $47.860 \pm 0.041$  Ma ( $2\sigma$ ). Visual inspection of the histogram in Figure 4a reveals that the Monte Carlo trials closely approximate a normal distribution. The mean and twice the standard deviation of the  $10^6$  trials yields  $47.860 \pm 0.041$  Ma ( $2\sigma$ ), agreeing to the numerical precision represented by two significant figures in the reported uncertainty. The  $^{207}\text{Pb}/^{235}\text{U}$  date for this analysis was also modeled by MCM, although this date is not usually reported in this age range because it is generally less precise. The Monte Carlo trials plotted in Figure 4b are also normally distributed, and the date calculated by U-Pb\_Redux and the Monte Carlo results both agree at  $48.12 \pm 0.33$  Ma ( $2\sigma$ ).

[116] The second analysis modeled is an Archean zircon with a Pb\*/Pbc of ~85 and measured  $^{206}\text{Pb}/^{205}\text{Pb}$  and  $^{207}\text{Pb}/^{205}\text{Pb}$  uncertainties of 0.022% and 0.029%, respectively. A histogram showing Monte Carlo evaluations of the  $^{207}\text{Pb}/^{206}\text{Pb}$  date is presented in Figure 4c, and approximates a normal distribution closely. The date and uncertainty of  $2576.0 \pm 1.5$  ( $2\sigma$ ) calculated by U-Pb\_Redux again agree with the mean and two standard deviations of the  $10^6$  Monte Carlo realizations within numerical precision.

[117] Finally, a <1 Ma zircon from the Bishop Tuff with a Pb\*/Pbc of 4.6 and a measured  $^{206}\text{Pb}/^{205}\text{Pb}$  uncertainty of 0.054% was modeled with MCM. For an analysis this young, the uncertainties in the  $^{230}\text{Th}$  correction (Appendix A) dominate the uncertainty budget. Here, the Th/U of the magma was assumed to have the same variability as Th/U ratios measured in melt inclusions in quartz phenocrysts,  $2.81 \pm 0.32$  ( $2\sigma$ ) [Crowley *et al.*, 2007]. Visual inspection of the histogram in Figure 4d reveals a distribution slightly skewed to the left. This results from a nonlinearity in the  $^{230}\text{Th}$  correction: Monte Carlo trials with lower magma Th/U values result in a range of Th corrections, rather than trials with higher Th/U magma values where the near-maximum correction is made. The linear uncertainty propagation algorithm employed by U-Pb\_Redux, calculates a  $^{230}\text{Th}$ -corrected  $^{206}\text{Pb}/^{238}\text{U}$  date of  $768.6 \pm 3.3$  ka ( $2\sigma$ ). This is approximated closely by the mean and symmetric 95% confidence interval calculated from the Monte Carlo realizations of  $768.5 \pm 3.3$  ka, with a difference between the expected values of only 78 years.

## 7. Conclusions

[118] We propose that the ID-TIMS community adopt a common U-Pb data reduction and uncertainty propagation algorithm for reporting, comparing, and archiving a rapidly growing amount of isotopic data. An ideal algorithm must provide a transparent model to calculate dates from input measurement, tracer, and laboratory parameters for a variety of tracers and for phases with and without initial common Pb, incorporating initial daughter product disequilibrium corrections. This model should also propagate the uncertainties in each input parameter, as well as any possible correlations between them, to determine the uncertainties and correlations between the variety of output isotopic ratios and dates geochronologists plot and interpret. Finally, a mechanism is required for combining several analyses into a single maximum likelihood

estimate of the date and uncertainty they represent, incorporating random and multiple systematic uncertainties.

[119] A new set of data reduction and uncertainty estimation algorithms fulfill these criteria and are embedded in the open source software package U-Pb\_Redux. Uncertainty propagation using the linear algebraic expression of covariance and Jacobian matrices is highly extensible, so that relationships between inputs, intermediate parameters, and outputs are easily codified and calculations are computationally inexpensive. This approach also determines the dependence of each measurement on often complexly related systematic uncertainties. If these systematic uncertainties are expressed as correlations between the dates being averaged, then the same linear algebraic uncertainty propagation techniques can be used to calculate the weighted mean dates and statistics.

[120] Interpreting uncertainties propagated linearly as confidence intervals assumes the model is linear at the scale of the input uncertainties. This assumption is tested and verified with Monte Carlo simulations of three typical zircon analyses, which show that typical ID-TIMS uncertainties yield normal distributions that agree with linear uncertainty propagation calculations.

## Appendix A: Disequilibrium Corrections and Initial Common Pb Models

[121] The U-Pb data reduction equations presented in section 2 assume that one daughter atom of  $^{206}\text{Pb}$  or  $^{207}\text{Pb}$  is created from the decay of each parent atom of  $^{238}\text{U}$  or  $^{235}\text{U}$ , respectively. However, the path from U to Pb in each system proceeds through a series of alpha and beta decays that produce a chain of intermediate daughter nuclides before yielding a Pb atom. The U-series decay chain is at ‘secular equilibrium’ when all isotopes have the same activity (equal to its decay constant multiplied by its atomic abundance), so that each intermediate daughter is being created from the nuclide before it in the chain at the same rate as it is decaying to the next daughter nuclide. This results in a higher abundance of daughter nuclides with longer half lives. Chemical processes that fractionate the parent and intermediate daughter nuclides disturb the secular equilibrium abundance ratios, creating intermediate daughter product disequilibrium.

[122] For instance, the elements U and Th are fractionated during crystallization of a dated phase if

their distribution coefficients in that phase differ (i.e.,  $D_{\text{Th}} \neq D_{\text{U}}$ ). This affects the longest-lived intermediate daughter product in the  $^{238}\text{U}$  decay chain,  $^{230}\text{Th}$  ( $t_{1/2} \approx 76$  kyr). Th is relatively incompatible compared to U during crystallization of zircon, for example, resulting in a  $^{230}\text{Th}$  deficiency, and it is relatively compatible in monazite, resulting in  $^{230}\text{Th}$  excess [Mattinson, 1973; Schärer, 1984]. In order for the  $^{230}\text{Th}$  to return to secular equilibrium, it must accumulate at the expense of  $^{206}\text{Pb}$  production in zircon or decay back to secular equilibrium levels in monazite, generating excess  $^{206}\text{Pb}$ . The resulting age correction for zircon is bounded: if Th is completely excluded from the crystal, the maximum correction of  $1/\lambda_{230} \approx 110$  kyr is made to the  $^{206}\text{Pb}/^{238}\text{U}$  date. However, if the mineral incorporates excess  $^{230}\text{Th}$ , then no upper bound exists on the theoretical magnitude of the age correction.

### A1. Th Correction Derivation

[123] Initial  $^{230}\text{Th}$  disequilibrium in the  $^{238}\text{U}$  decay chain necessitates a correction to the molar quantity of  $^{206}\text{Pb}$  in the conventional age equation,  $D = P(e^{\lambda t} - 1)$ :

$$\begin{aligned} \text{moles}(^{206}\text{Pb})_{\text{rad}} = & \text{moles}(^{238}\text{U})_{\text{spl}} \cdot \left( e^{\lambda_{238} t_{206/238}^{\text{Th}}} - 1 \right) \\ & + \text{moles}(^{230}\text{Th})_{\text{init}} - \text{moles}(^{230}\text{Th})_{\text{eqbm}} \end{aligned} \quad (\text{A1})$$

where  $t_{206/238}^{\text{Th}}$  is the  $^{206}\text{Pb}/^{238}\text{U}$  date of the sample corrected for initial  $^{230}\text{Th}$  disequilibrium. The difference between the moles of  $^{230}\text{Th}$  at initial crystallization and the moles of  $^{230}\text{Th}$  at secular equilibrium is negative if Th has been excluded from the mineral, decreasing the moles of  $^{206}\text{Pb}$  subsequently produced, or positive if Th has been preferentially included into the mineral, generating excess  $^{206}\text{Pb}$ .

[124] Molar quantities in equation (A1) can be expressed as isotopic abundance ratios by dividing through by the moles of parent isotope,  $^{238}\text{U}$ . Due to the long half-life of  $^{238}\text{U}$  ( $\sim 4.5$  Gyr), its atomic abundance is assumed to be the same at crystallization and after returning to secular equilibrium, which occurs after about six half lives of the longest lived intermediate daughter, or  $\sim 460$  kyr, if all  $^{230}\text{Th}$  is excluded.

$$\left( \frac{^{206}\text{Pb}}{^{238}\text{U}} \right)_{\text{rad}} = e^{\lambda_{238} t_{206/238}^{\text{Th}}} - 1 + \left( \frac{^{230}\text{Th}}{^{238}\text{U}} \right)_{\text{init}} - \left( \frac{^{230}\text{Th}}{^{238}\text{U}} \right)_{\text{eqbm}} \quad (\text{A2})$$

[125] The Th/U ratios on the right-hand side of equation (A2) can be expressed as activity ratios by multiplying the atomic abundance of each isotope by its decay constant. Equality is maintained by multiplying the resulting expression by the reciprocal of the decay constant ratio.

$$\begin{aligned} & \left( \frac{^{230}\text{Th}}{^{238}\text{U}} \right)_{\text{init}} - \left( \frac{^{230}\text{Th}}{^{238}\text{U}} \right)_{\text{eqbm}} \\ & = \frac{\lambda_{238}}{\lambda_{230}} \left( \frac{\lambda_{230}}{\lambda_{238}} \left( \frac{^{230}\text{Th}}{^{238}\text{U}} \right)_{\text{init}} - \frac{\lambda_{230}}{\lambda_{238}} \left( \frac{^{230}\text{Th}}{^{238}\text{U}} \right)_{\text{eqbm}} \right) \\ & = \frac{\lambda_{238}}{\lambda_{230}} \left( \left[ \frac{^{230}\text{Th}}{^{238}\text{U}} \right]_{\text{init}} - \left[ \frac{^{230}\text{Th}}{^{238}\text{U}} \right]_{\text{eqbm}} \right) \end{aligned} \quad (\text{A3})$$

where the square brackets enclose activity ratios.

[126] Both activity ratios in expression (A3) may be transformed into measurable parameters. The degree of initial isotopic disequilibrium depends on the ratio between the distribution coefficients  $D_{\text{Th}}$  and  $D_{\text{U}}$ . Each distribution coefficient describes the ratio of the molar abundance of Th and U in the sample to the molar abundance in the magma. This expression can be rearranged so that the abundance ratio of sample isotopes is in the numerator and the corresponding magma abundance ratio is in the denominator.

$$\frac{D_{\text{Th}}}{D_{\text{U}}} = \frac{\text{Th}_{\text{spl}}/\text{Th}_{\text{magma}}}{\text{U}_{\text{spl}}/\text{U}_{\text{magma}}} = \frac{(\text{Th}/\text{U})_{\text{spl}}}{(\text{Th}/\text{U})_{\text{magma}}} \quad (\text{A4})$$

Fractionation of specific isotopes, such as  $^{230}\text{Th}$  and  $^{238}\text{U}$ , follow the same rule, yielding an equivalent expression in terms of the initial molar  $^{230}\text{Th}/^{238}\text{U}$  ratio of the sample and the magma. The molar ratio can again be converted to an activity ratio by multiplying each isotope by its decay constant.

$$\frac{(\text{Th}/\text{U})_{\text{spl}}}{(\text{Th}/\text{U})_{\text{magma}}} = \frac{\left( \frac{^{230}\text{Th}/^{238}\text{U}} \right)_{\text{init}}}{\left( \frac{^{230}\text{Th}/^{238}\text{U}} \right)_{\text{magma}}} \cdot \frac{\lambda_{230}/\lambda_{238}}{\lambda_{230}/\lambda_{238}} \quad (\text{A5})$$

The numerator and denominator become activity ratios, denoted by square brackets. Assuming that the magma is at secular equilibrium at crystallization, its activity ratio  $\left[ \frac{^{230}\text{Th}}{^{238}\text{U}} \right]_{\text{magma}} = 1$ .

$$\frac{(\text{Th}/\text{U})_{\text{spl}}}{(\text{Th}/\text{U})_{\text{magma}}} = \frac{\left[ \frac{^{230}\text{Th}}{^{238}\text{U}} \right]_{\text{init}}}{\left[ \frac{^{230}\text{Th}}{^{238}\text{U}} \right]_{\text{magma}}} = \left[ \frac{^{230}\text{Th}}{^{238}\text{U}} \right]_{\text{init}} \quad (\text{A6})$$

Thus, the initial  $\left[ \frac{^{230}\text{Th}}{^{238}\text{U}} \right]$  activity ratio is equivalent to the ratio of distribution coefficients

$D_{Th}/D_U$ , and the Th/U of the sample divided by the Th/U of the magma. Instead of assuming the magma to be at secular equilibrium, both may be multiplied by the  $[^{230}Th/^{238}U]$  activity ratio of the magma to yield the initial  $[^{230}Th/^{238}U]$  activity ratio at crystallization if constraints exist on its value.

[127] Finally, the  $[^{230}Th/^{238}U]$  activity ratio of the sample after it has attained secular equilibrium is also equal to one,

$$\left[ \frac{^{230}Th}{^{238}U} \right]_{eqbm} = 1 \quad (A7)$$

[128] Substituting the recast activity ratios in (A6) and (A7) into (A3), then substituting this expression into (A2) yields the conventional equation for the  $^{230}Th$ -corrected  $^{206}Pb/^{238}U$  date [e.g., Schärer, 1984],

$$\left( \frac{^{206}Pb}{^{238}U} \right)_{rad} = e^{\lambda_{238} \cdot t_{206/238}^{Th}} - 1 + \frac{\lambda_{238}}{\lambda_{230}} \cdot \left[ \left( \frac{Th}{U} \right)_{spl} / \left( \frac{Th}{U} \right)_{magma} - 1 \right] \quad (A8)$$

[129] Alternately, if the ratio of distribution coefficients  $D_{Th}/D_U$  is better constrained than the Th/U of the magma, the left side of equation (A4) can be substituted into equation (A8),

$$\left( \frac{^{206}Pb}{^{238}U} \right)_{rad} = e^{\lambda_{238} \cdot t_{206/238}^{Th}} - 1 + \frac{\lambda_{238}}{\lambda_{230}} \cdot \left( \frac{D_{Th}}{D_U} - 1 \right) \quad (A9)$$

## A2. Th Correction Implementation

[130] In order to calculate the  $^{230}Th$ -corrected  $^{206}Pb/^{238}U$  date in equation (A8), an estimate of the Th/U of the magma is required; the Th/U of the sample may be calculated from available data. Because the Th/U of the magma is expressed as an atomic abundance ratio, the total atomic abundances of Th and U in the sample are required, which are each the sum of the abundances of the respective major isotopes. The atomic abundance of U in the sample,  $moles(U)_{spl}$ , is the sum of the moles of  $^{238}U$  and  $^{235}U$ ,

$$moles(U)_{spl} = moles(^{238}U)_{spl} + moles(^{235}U)_{spl} \quad (A10)$$

[131] The element Th has a single major isotope,  $^{232}Th$ ; the second largest contribution, from the  $^{230}Th$  in the  $^{238}U$  decay chain, is negligible. Due to the long half-life of  $^{232}Th$  (~14 Gyr), there is no significant difference between the abundance of Th

at present and during crystallization. The atomic abundance of  $^{232}Th$  in the sample can be back-calculated from the moles of radiogenic  $^{208}Pb$  derived in equation (23) and the  $^{230}Th$ -corrected date of the sample. The moles of  $^{232}Th$  in the sample is given by a rearrangement of the isotopic decay equation,  $D/P = e^{\lambda t} - 1$ ,

$$moles(^{232}Th)_{spl} = \frac{moles(^{208}Pb)_{rad}}{\exp(\lambda_{232} \cdot t_{206/238}^{Th}) - 1} \quad (A11)$$

where  $t_{206/238}^{Th}$  is the  $^{230}Th$ -corrected  $^{206}Pb/^{238}U$  date.

[132] The expressions in (A10) and (A11) can be substituted into equation (A8) to yield a new equation

$$\left( \frac{^{206}Pb}{^{238}U} \right)_{rad} = e^{\lambda_{238} \cdot t_{206/238}^{Th}} - 1 + \frac{\lambda_{238}}{\lambda_{230}} \cdot \left[ \frac{moles(^{208}Pb)_{rad} / (e^{\lambda_{232} \cdot t_{206/238}^{Th}} - 1)}{moles(U)_{spl}} / \left( \frac{Th}{U} \right)_{magma} - 1 \right] \quad (A12)$$

This equation cannot be solved directly for  $t_{206/238}^{Th}$ , so U-Pb\_Redux utilizes Newton's Method, an iterative numerical solution.

[133] Alternately, equation (A9) can be solved directly for  $t_{206/238}^{Th}$  if the ratio of distribution coefficients is known,

$$t_{206/238}^{Th} = \frac{1}{\lambda_{238}} \log \left[ \left( \frac{^{206}Pb}{^{238}U} \right)_{rad} + 1 - \frac{\lambda_{238}}{\lambda_{230}} \left( \frac{D_{Th}}{D_U} - 1 \right) \right] \quad (A13)$$

[134] Using the  $^{230}Th$ -corrected  $^{206}Pb/^{238}U$  date calculated in equation (A12) or (A13), it is possible to calculate the moles of  $^{232}Th$  in the sample (equation (A11)), as well as the Th-corrected moles of  $^{206}Pb$ ,

$$moles(^{206}Pb)_{rad}^{Th} = moles(^{238}U)_{spl} \cdot (e^{\lambda_{238} \cdot t_{206/238}^{Th}} - 1) \quad (A14)$$

and the Th-corrected  $^{206}Pb/^{238}U$  ratio used in the conventional concordia plot,

$$\left( \frac{^{206}Pb}{^{238}U} \right)_{rad}^{Th} = \frac{moles(^{206}Pb)_{rad}^{Th}}{moles(^{238}U)_{spl}} \quad (A15)$$

[135] A  $^{230}Th$  correction is most often applied to samples younger than ca. 500 Ma, whose uncertainties are comparable to the magnitude of the

correction. The  $^{207}\text{Pb}/^{206}\text{Pb}$  date is not often used for young (<ca. 2 Ga) samples because it is sensitive to the low abundance of  $^{207}\text{Pb}$  in young samples. However, *Amelin et al.* [2010] show that evolving laboratory and mass spectrometry techniques applied to early solar system studies offer ever-finer resolving power at >4.5 Ga suggesting that Th correction may become necessary. The  $^{230}\text{Th}$ -corrected radiogenic  $^{207}\text{Pb}/^{206}\text{Pb}$  ratio is

$$\left(\frac{^{207}\text{Pb}}{^{206}\text{Pb}}\right)_{rad}^{Th} = \frac{\text{moles}(^{207}\text{Pb})_{rad}}{\text{moles}(^{206}\text{Pb})_{rad}^{Th}} \quad (\text{A16})$$

As with the un-corrected  $^{207}\text{Pb}/^{206}\text{Pb}$  date, a solution for  $t_{207/206}^{Th}$  cannot be reached analytically for the equation

$$\left(\frac{^{207}\text{Pb}}{^{206}\text{Pb}}\right)_{rad}^{Th} = \left(\frac{^{238}\text{U}}{^{235}\text{U}}\right)_{spl}^{-1} \cdot \frac{\exp(\lambda_{235} \cdot t_{207/206}^{Th}) - 1}{\exp(\lambda_{238} \cdot t_{207/206}^{Th}) - 1} \quad (\text{A17})$$

Instead, Newton's Method is employed by U-Pb\_Redux.

### A3. Pa Correction

[136] The longest-lived intermediate daughter product in the  $^{235}\text{U}$  decay chain is  $^{231}\text{Pa}$ , with a half-life of ~33 kyr. Analogous to  $^{230}\text{Th}$  in the  $^{238}\text{U}$  decay chain, the  $[^{231}\text{Pa}/^{235}\text{U}]$  activity ratio may be perturbed during crystallization from a magma at secular equilibrium. Unlike the  $^{230}\text{Th}$  correction, however, there is no way to back-calculate the initial Pa/U ratio of the dated phase, as with the  $^{208}\text{Pb}$  daughter of  $^{232}\text{Th}$  in equation (A12). Instead, correction requires the initial  $[^{231}\text{Pa}/^{235}\text{U}]$  activity ratio at crystallization or  $D_{\text{Pa}}/D_{\text{U}}$ , the ratio of the Pa and U distribution coefficients in the dated phase. Derivation of the  $^{231}\text{Pa}$  correction equations parallels the  $^{230}\text{Th}$  equations presented above.

[137] The  $^{231}\text{Pa}$ -corrected  $^{207}\text{Pb}/^{235}\text{U}$  date,  $t_{207/235}^{Pa}$ , can be calculated in the same manner as equation (A13).

$$t_{207/235}^{Pa} = \frac{1}{\lambda_{235}} \log \left[ \left(\frac{^{207}\text{Pb}}{^{235}\text{U}}\right)_{rad} + 1 - \frac{\lambda_{235}}{\lambda_{231}} \left( \left[\frac{^{231}\text{Pa}}{^{235}\text{U}}\right]_{spl} - 1 \right) \right] \quad (\text{A18})$$

[138] Likewise,  $^{231}\text{Pa}$ -corrected moles of  $^{207}\text{Pb}$  can be calculated using the corrected  $^{207}\text{Pb}/^{235}\text{U}$  date,

$$\text{moles}(^{207}\text{Pb})_{rad}^{Pa} = \text{moles}(^{235}\text{U})_{spl} \left( e^{\lambda_{235} \cdot t_{207/235}^{Pa}} - 1 \right) \quad (\text{A19})$$

and then used to calculate the  $^{231}\text{Pa}$ -corrected radiogenic  $^{207}\text{Pb}/^{206}\text{Pb}$  ratio,

$$\left(\frac{^{207}\text{Pb}}{^{206}\text{Pb}}\right)_{rad}^{Pa} = \frac{\text{moles}(^{207}\text{Pb})_{rad}^{Pa}}{\text{moles}(^{206}\text{Pb})_{rad}} \quad (\text{A20})$$

and the  $^{231}\text{Pa}$ -corrected radiogenic  $^{207}\text{Pb}/^{235}\text{U}$  ratio,

$$\left(\frac{^{207}\text{Pb}}{^{235}\text{U}}\right)_{rad}^{Pa} = \frac{\text{moles}(^{207}\text{Pb})_{rad}^{Pa}}{\text{moles}(^{235}\text{U})_{spl}} \quad (\text{A21})$$

for Tera-Wasserburg and conventional concordia plots.

[139] To calculate a  $^{231}\text{Pa}$ -corrected  $^{207}\text{Pb}/^{206}\text{Pb}$  date, it is not possible to solve

$$\left(\frac{^{207}\text{Pb}}{^{206}\text{Pb}}\right)_{rad}^{Pa} = \left(\frac{^{238}\text{U}}{^{235}\text{U}}\right)_{spl}^{-1} \cdot \frac{\exp(\lambda_{235} \cdot t_{207/206}^{Pa}) - 1}{\exp(\lambda_{238} \cdot t_{207/206}^{Pa}) - 1} \quad (\text{A22})$$

directly for  $t_{207/206}^{Pa}$ . Instead, an iterative numerical solution such as Newton's Method must be employed.

### A4. Simultaneous Th Correction and Pa Correction

[140] Finally, the  $^{207}\text{Pb}/^{206}\text{Pb}$  ratio and date may be corrected for both  $^{230}\text{Th}$  and  $^{231}\text{Pa}$  disequilibrium using equations (A14) and (A19).

$$\left(\frac{^{207}\text{Pb}}{^{206}\text{Pb}}\right)_{rad}^{ThPa} = \frac{\text{moles}(^{207}\text{Pb})_{rad}^{Pa}}{\text{moles}(^{206}\text{Pb})_{rad}^{Th}} \quad (\text{A23})$$

[141] To calculate a  $^{230}\text{Th}$ - and  $^{231}\text{Pa}$ -corrected  $^{207}\text{Pb}/^{206}\text{Pb}$  date, it is not possible to solve

$$\left(\frac{^{207}\text{Pb}}{^{206}\text{Pb}}\right)_{rad}^{ThPa} = \left(\frac{^{238}\text{U}}{^{235}\text{U}}\right)_{spl}^{-1} \cdot \frac{\exp(\lambda_{235} \cdot t_{207/206}^{ThPa}) - 1}{\exp(\lambda_{238} \cdot t_{207/206}^{ThPa}) - 1} \quad (\text{A24})$$

in terms of  $t_{207/206}^{ThPa}$ . Instead, an iterative numerical solution is used.

### A5. Initial Common Pb Correction

[142] Following [*Stacey and Kramers, 1975*], for fractions with estimated dates between 4.57 and 3.7 Ga,

$$\left(\frac{^{206}\text{Pb}}{^{204}\text{Pb}}\right)_{com} = 7.19 \cdot \left[ e^{(\lambda_{238} \cdot 4.57 \times 10^9)} - e^{(\lambda_{238} \cdot t_{\text{Pbc}})} \right] + 9.307 \quad (\text{A25})$$



$$\left(\frac{^{207}\text{Pb}}{^{204}\text{Pb}}\right)_{\text{com}} = \frac{7.19}{137.88} \cdot \left[ e^{(\lambda_{235} \cdot 4.57 \times 10^9)} - e^{(\lambda_{235} \cdot t_{\text{Pbc}})} \right] + 10.294 \quad (\text{A26})$$

$$\left(\frac{^{208}\text{Pb}}{^{204}\text{Pb}}\right)_{\text{com}} = 33.21 \cdot \left[ e^{(\lambda_{232} \cdot 4.57 \times 10^9)} - e^{(\lambda_{232} \cdot t_{\text{Pbc}})} \right] + 29.487 \quad (\text{A27})$$

and for fractions younger than 3.7 Ga,

$$\left(\frac{^{206}\text{Pb}}{^{204}\text{Pb}}\right)_{\text{com}} = 9.74 \cdot \left[ e^{(\lambda_{238} \cdot 3.7 \times 10^9)} - e^{(\lambda_{238} \cdot t_{\text{Pbc}})} \right] + 11.152 \quad (\text{A28})$$

$$\left(\frac{^{207}\text{Pb}}{^{204}\text{Pb}}\right)_{\text{com}} = \frac{9.74}{137.88} \cdot \left[ e^{(\lambda_{235} \cdot 3.7 \times 10^9)} - e^{(\lambda_{235} \cdot t_{\text{Pbc}})} \right] + 12.998 \quad (\text{A29})$$

$$\left(\frac{^{208}\text{Pb}}{^{204}\text{Pb}}\right)_{\text{com}} = 36.84 \cdot \left[ e^{(\lambda_{232} \cdot 3.7 \times 10^9)} - e^{(\lambda_{232} \cdot t_{\text{Pbc}})} \right] + 31.23 \quad (\text{A30})$$

## Acknowledgments

[143] This research was made possible by grants EAR-0746205 and EAR-0930166 from the National Science Foundation. The manuscript benefitted from insightful comments by Blair Schoene and Dan Condon and helpful formal reviews from Mark Schmitz and Don Davis.

## References

- Amelin, Y., A. N. Krot, I. D. Hutcheon, and A. A. Ulyanov (2002), Lead isotopic ages of chondrules and calcium-aluminum-rich inclusions, *Science*, *297*(5587), 1678–1683, doi:10.1126/science.1073950.
- Amelin, Y., A. Kaltenbach, T. Iizuka, C. H. Stirling, T. R. Ireland, M. Petaev, and S. B. Jacobsen (2010), U-Pb chronology of the Solar System's oldest solids with variable  $^{238}\text{U}/^{235}\text{U}$ , *Earth Planet. Sci. Lett.*, *300*(3–4), 343–350, doi:10.1016/j.epsl.2010.10.015.
- BIPM, IEC, IFCC, ISO, IUPAC, IUPAP, and OIML (2008a), Evaluation of measurement data—Guide to the Expression of Uncertainty in Measurement, *JCGM 100*, Int. Organ. for Stand., Geneva, Switz.
- BIPM, IEC, IFCC, ILAC, ISO, IUPAC, IUPAP, and OIML (2008b), Evaluation of measurement data—Supplement to the “Guide to the Expression of Uncertainty in Measurement”—Propagation of distributions using a Monte Carlo method, *JCGM 101*, Int. Organ. for Stand., Geneva, Switz.
- Bowring, J. F., N. M. McLean, and S. A. Bowring (2011), Engineering cyber infrastructure for U-Pb geochronology: Tripoli and U-Pb\_Redux, *Geochem. Geophys. Geosyst.*, doi:10.1029/2010GC003478, in press.
- Bowring, S. A., D. H. Erwin, Y. G. Jin, M. W. Martin, K. Davidek, and W. Wang (1998), U/Pb zircon geochronology and tempo of the end-Permian mass extinction, *Science*, *280*(5366), 1039–1045, doi:10.1126/science.280.5366.1039.
- Brennecke, G. A., S. Weyer, M. Wadhwa, P. E. Janney, J. Zipfel, and A. D. Anbar (2010),  $^{238}\text{U}/^{235}\text{U}$  variations in meteorites: Extant  $^{247}\text{Cm}$  and implications for Pb-Pb dating, *Science*, *327*(5964), 449–451, doi:10.1126/science.1180871.
- Briqueu, L., and H. de la Boisse (1990), U-Pb geochronology: Systematic development of mixing equations and application of Monte Carlo numerical simulation to the error propagation in the Concordia diagram, *Chem. Geol.*, *88*(1–2), 69–83, doi:10.1016/0009-2541(90)90104-F.
- Cox, M. G., and B. R. L. Siebert (2006), The use of a Monte Carlo method for evaluating uncertainty and expanded uncertainty, *Metrologia*, *43*, S178, doi:10.1088/0026-1394/43/4/S03.
- Crowley, J. L., B. Schoene, and S. A. Bowring (2007), U-Pb dating of zircon in the Bishop Tuff at the millennial scale, *Geology*, *35*(12), 1123–1126, doi:10.1130/G24017A.1.
- Cumming, G. L., and J. R. Richards (1975), Ore lead isotope ratios in a continuously changing Earth, *Earth Planet. Sci. Lett.*, *28*(2), 155–171, doi:10.1016/0012-821X(75)90223-X.
- Davydov, V. I., J. L. Crowley, M. D. Schmitz, and V. I. Poletaev (2010), High-precision U-Pb zircon age calibration of the global Carboniferous time scale and Milankovitch band cyclicity in the Donets basin, eastern Ukraine, *Geochem. Geophys. Geosyst.*, *11*, Q0AA04, doi:10.1029/2009GC002736.
- Dempster, A. P., N. M. Laird, and D. B. Rubin (1977), Maximum likelihood from incomplete data via the EM algorithm, *J. R. Stat. Soc., Ser. B*, *39*(1), 1–38.
- Housh, T., and S. A. Bowring (1991), Lead isotopic heterogeneities within alkali feldspars: Implications for the determination of initial lead isotopic compositions, *Geochim. Cosmochim. Acta*, *55*(8), 2309–2316, doi:10.1016/0016-7037(91)90106-F.
- Ludwig, K. (1980), Calculation of uncertainties of U-Pb isotope data, *Earth Planet. Sci. Lett.*, *46*(2), 212–220, doi:10.1016/0012-821X(80)90007-2.
- Ludwig, K. (1998), On the treatment of concordant uranium-lead ages, *Geochim. Cosmochim. Acta*, *62*(4), 665–676, doi:10.1016/S0016-7037(98)00059-3.
- Ludwig, K. (2009), Errors of isotope ratios acquired by double interpolation, *Chem. Geol.*, *268*(1–2), 24–26, doi:10.1016/j.chemgeo.2009.07.004.
- Lyons, L., D. Gibaut, and P. Clifford (1988), How to combine correlated estimates of a single physical quantity, *Nucl. Instrum. Methods Phys. Res., Sect. A*, *270*(1), 110–117, doi:10.1016/0168-9002(88)90018-6.
- Mattinson, J. M. (1973), Anomalous isotopic composition of lead in young zircons, *Year Book Carnegie Inst. Washington*, *72*, 613–616.
- Mattinson, J. M. (2005), Zircon U-Pb chemical abrasion (“CA-TIMS”) method: Combined annealing and multi-step partial dissolution analysis for improved precision and accuracy of zircon ages, *Chem. Geol.*, *220*(1–2), 47–66, doi:10.1016/j.chemgeo.2005.03.011.
- Mattinson, J. M. (2010), Analysis of the relative decay constants of  $^{235}\text{U}$  and  $^{238}\text{U}$  by multi-step CA-TIMS measurements of closed-system natural zircon samples, *Chem. Geol.*, *275*(3–4), 186–198, doi:10.1016/j.chemgeo.2010.05.007.
- Moorbath, S., P. N. Taylor, J. L. Orpen, P. Treloar, and J. F. Wilson (1987), First direct radiometric dating of Archaean stromatolitic limestone, *Nature*, *326*(6116), 865–867, doi:10.1038/326865a0.

- Patterson, C. (1956), Age of meteorites and the Earth, *Geochim. Cosmochim. Acta*, *10*(4), 230–237, doi:10.1016/0016-7037(56)90036-9.
- Roddick, J. C. (1987), Generalized numerical error analysis with applications to geochronology and thermodynamics, *Geochim. Cosmochim. Acta*, *51*(8), 2129–2135.
- Scaillet, S. (2000), Numerical error analysis in  $^{40}\text{Ar}/^{39}\text{Ar}$  dating, *Chem. Geol.*, *162*(3–4), 269–298, doi:10.1016/S0009-2541(99)00149-7.
- Schärer, U. (1984), The effect of initial  $^{230}\text{Th}$  disequilibrium on young U-Pb ages: the Makalu case, Himalaya, *Earth Planet. Sci. Lett.*, *67*(2), 191–204, doi:10.1016/0012-821X(84)90114-6.
- Schmitz, M. D., and B. Schoene (2007), Derivation of isotope ratios, errors, and error correlations for U-Pb geochronology using  $^{205}\text{Pb}$ - $^{235}\text{U}$ -( $^{233}\text{U}$ )-spiked isotope dilution thermal ionization mass spectrometric data, *Geochem. Geophys. Geosyst.*, *8*, Q08006, doi:10.1029/2006GC001492.
- Schoene, B., and S. Bowring (2006), U-Pb systematics of the McClure Mountain syenite: thermochronological constraints on the age of the  $^{40}\text{Ar}/^{39}\text{Ar}$  standard MMhb, *Contrib. Mineral. Petrol.*, *151*(5), 615–630, doi:10.1007/s00410-006-0077-4.
- Schoene, B., J. L. Crowley, D. J. Condon, M. D. Schmitz, and S. A. Bowring (2006), Reassessing the uranium decay constants for geochronology using ID-TIMS U-Pb data, *Geochim. Cosmochim. Acta*, *70*(2), 426–445, doi:10.1016/j.gca.2005.09.007.
- Schoene, B., M. J. de Wit, and S. A. Bowring (2008), Mesoarchean assembly and stabilization of the eastern Kaapvaal craton: A structural-thermochronological perspective, *Tectonics*, *27*, TC5010, doi:10.1029/2008TC002267.
- Stacey, J., and J. Kramers (1975), Approximation of terrestrial lead isotope evolution by a two-stage model, *Earth Planet. Sci. Lett.*, *26*(2), 207–221, doi:10.1016/0012-821X(75)90088-6.
- Steiger, R., and E. Jäger (1977), Subcommittee on geochronology: Convention on the use of decay constants in geo- and cosmochronology, *Earth Planet. Sci. Lett.*, *36*(3), 359–362, doi:10.1016/0012-821X(77)90060-7.
- Stirling, C. H., M. B. Andersen, E.-K. Potter, and A. N. Halliday (2007), Low-temperature isotopic fractionation of uranium, *Earth Planet. Sci. Lett.*, *264*(1–2), 208–225, doi:10.1016/j.epsl.2007.09.019.
- Valassi, A. (2003), Combining correlated measurements of several different physical quantities, *Nucl. Instrum. Methods Phys. Res., Sect. A*, *500*(1–3), 391–405, doi:10.1016/S0168-9002(03)00329-2.
- Wendt, I., and C. Carl (1991), The statistical distribution of the mean squared weighted deviation, *Chem. Geol.*, *86*(4), 275–285, doi:10.1016/0168-9622(91)90010-T.
- Weyer, S., A. D. Anbar, A. Gerdes, G. W. Gordon, T. J. Algeo, and E. A. Boyle (2008), Natural fractionation of  $^{238}\text{U}/^{235}\text{U}$ , *Geochim. Cosmochim. Acta*, *72*(2), 345–359, doi:10.1016/j.gca.2007.11.012.